

## Intrinsic growth and microzooplankton grazing on toxigenic *Pseudo-nitzschia* spp. diatoms from the coastal northeast Pacific

M. Brady Olson<sup>1</sup> and Evelyn J. Lessard

School of Oceanography, University of Washington, Seattle, Washington 98195

William P. Cochlan

Romberg Tiburon Center for Environmental Studies, San Francisco State University, Tiburon, California 94920

Vera L. Trainer

National Oceanic and Atmospheric Administration (NOAA) Fisheries, Marine Biotoxins Program, Environmental Conservation Division, Northwest Fisheries Science Center, Seattle, Washington 98112

### Abstract

We investigated the population ecology of toxigenic diatoms within the genus *Pseudo-nitzschia* on the Pacific Northwest coast during 2003, 2004, and 2005. *Pseudo-nitzschia* spp. were widespread and abundant across the region, and the maximum density reached at our experimental stations was  $\sim 7 \times 10^6$  cells L<sup>-1</sup>. *Pseudo-nitzschia* spp. biomass did not correlate with total phytoplankton biomass, indicating that the growth response and/or mortality rate of *Pseudo-nitzschia* spp. were dissimilar to other phytoplankton. In dilution experiments across wide-ranging ocean conditions, *Pseudo-nitzschia* spp. intrinsic growth rates were moderate to high ( $\bar{x} = 0.97$  d<sup>-1</sup>, range 0.24 d<sup>-1</sup> to 2.30 d<sup>-1</sup>,  $n = 36$ ), and they were consistently higher than the corresponding growth rates of the aggregate <5- $\mu$ m and >5- $\mu$ m chlorophyll *a* (Chl *a*) communities. *Pseudo-nitzschia* spp. growth was predicted by irradiance and temperature but not ambient nitrate concentration, whereas both Chl *a* size fractions showed dependence upon nitrate for growth. Microzooplankton grazing rates on *Pseudo-nitzschia* spp. were moderate ( $\bar{x} = 0.32$  d<sup>-1</sup>, range 0.00 d<sup>-1</sup> to 1.70 d<sup>-1</sup>,  $n = 36$ ); they were nearly always lower than corresponding *Pseudo-nitzschia* spp. intrinsic growth, significantly lower than the grazing rates on the <5- $\mu$ m Chl *a* size fraction, and comparable to grazing rates on the >5- $\mu$ m Chl *a* size fraction. Our results show that the strong competitive fitness of *Pseudo-nitzschia* spp. results more from expression of characteristics that enable sustained high growth during variable and unfavorable conditions than from intrinsic adaptations that reduce grazing mortality.

Waters off the coasts of Washington State, U.S.A., and Vancouver Island, Canada, are well known for the widespread presence and variable toxicity of at least eight species within the toxigenic diatom genus *Pseudo-nitzschia*

(*P-n*) (Horner et al. 2000; Stehr et al. 2002; Trainer et al. 2002). *P-n* spp. are widespread in this region (collectively known as the Pacific Northwest [PNW]) over time and space (Adams et al. 2000; Horner et al. 2000). The climatology, hydrography, and topography in this region of the PNW cooperate to create a dynamic and highly productive ecosystem (e.g., Hickey and Banas 2003). In particular, the seasonal cold-core Juan de Fuca eddy (MacFadyen et al. in press) is a retentive feature that often selects for high concentrations of both *P-n* spp. and its associated neurotoxin, domoic acid (DA) (Trainer et al. 2002). The ability of *P-n* spp. to thrive over time and space in this complex region indicates that they have the ability to tolerate wide-ranging environmental conditions. However, the most influential components governing the in situ population ecology of *P-n* spp. are not well understood.

*P-n* spp. are relatively unique diatoms because they are distributed globally (Bates and Trainer 2006 and reference therein), including regions far offshore (e.g., Marchetti et al. 2006a), albeit at low densities. In high nutrient, low chlorophyll (HNLC) regions, pennate diatoms such as *P-n* often become the numerically dominant diatom following the alleviation of Fe limitation during both shipboard and mesoscale Fe-enrichment experiments (e.g., Marchetti et al. 2006b and references therein).

*P-n* spp. are capable of forming dense blooms (Bates et al. 1998), and cell concentrations on the U.S. West Coast

<sup>1</sup> Corresponding author (bolson@marine.usf.edu). Present address: College of Marine Science, University of South Florida, St. Petersburg, Florida 33701.

### Acknowledgments

We thank J. Herndon (Romberg Tiburon Center for Environmental Studies, San Francisco State University) for providing nutrient data and K. Baugh and S. Nance (National Oceanic and Atmospheric Administration [NOAA], Northwest Fisheries Science Center) for providing domoic acid data. The assistance of M. Foy and M. Bernhardt (University of Washington) in the field and laboratory was instrumental for the success of this project. We thank all other members of the ECOHAB-PNW (Ecology of Harmful Algal Blooms–Pacific Northwest) team for their enthusiastic assistance with this work. This work would not have been possible if not for the assistance of the officers and crew of the research vessels *Wecoma*, *Atlantis*, and *Melville*. Finally, we wish to thank E. Frame (University of Washington) and two anonymous reviewers for their critiques of an earlier version of this manuscript. This work was conducted as part of the ECOHAB-PNW program and was funded by National Science Foundation grant OCE-0234587 and the Coastal Ocean Program of NOAA (NA170P2789). This is ECOHAB publication 248 and ECOHAB-PNW publication 15.

have been reported as high as  $10^7$  cells  $L^{-1}$  (Schnitzer et al. 2007 and references therein). Many members of the *P-n* genus have gained notoriety for their ability to produce the potent neurotoxin DA, which has been implicated as an agent of mortality for seabirds (Work et al. 1993), marine mammals (Scholin et al. 2000), and humans (Perl et al. 1990). With the capacity to produce a marine toxin, coupled with its oceanwide distribution and ability to accumulate to extremely high densities, *P-n* spp. are not only a globally significant phytoplankton in terms of biogeochemical cycling, but they also can have negative societal and ecological effects.

The temporal and spatial prevalence of *P-n* spp., both globally and in the PNW, suggests that this diatom may possess unique growth strategies that elevate its competitive fitness over other phytoplankton. Laboratory studies have shown that *P-n* spp. have superior or unique N (Auro 2007; Cochlan et al. in press) and Fe acquisition strategies (e.g., Rue and Bruland 2001; Maldonado et al. 2002; Marchetti et al. 2006a). However, apparent adaptations directed toward maximizing growth under variable—and perhaps unfavorable—growth conditions will only be effective if mortality rate is low relative to growth rate. As such, investment in adaptive strategies directed toward reducing mortality relative to growth may help to facilitate the accumulation of these diatoms to bloom densities.

The fate of most phytoplankton production is, arguably, mortality from zooplankton grazing (Banse 1994). Mounting evidence suggests that the most significant source of phytoplankton grazing mortality in the ocean is from microzooplankton (Calbet and Landry 2004). This is true not only for the open ocean, where typically small-sized cells dominate phytoplankton biomass seasonally (Frost 1991), but also for productive coastal ecosystems that are periodically diatom-dominated (e.g., Neuer and Cowles 1994; Strom et al. 2001). To date, however, no estimates of microzooplankton grazing on *P-n* spp. have been made, leaving a decidedly incomplete understanding of *P-n* spp. population ecology.

As part of the ECOHAB-PNW (Ecology and Oceanography of Harmful Algal Blooms—Pacific Northwest) project, we investigated the in situ population ecology of *P-n* spp. found off the PNW coast. Our goal was to determine the variables that most influence the growth and mortality of *P-n* spp. and, hence, control their distribution and abundance in this region. Further, we wished to determine whether the variables that influence *P-n* spp. population ecology act on other members of the phytoplankton community with equal magnitude. To that end, we measured intrinsic growth and microzooplankton grazing rates for *P-n* and size-fractionated chlorophyll *a* (Chl *a*) in 36 experiments performed during summer and fall cruises in 2003, 2004, and 2005. These experiments were conducted along and across the PNW continental shelf under widely varying hydrographic and nutrient conditions.

## Methods

*Station locations and sampling*—*P-n* spp. growth and microzooplankton grazing experiments were conducted

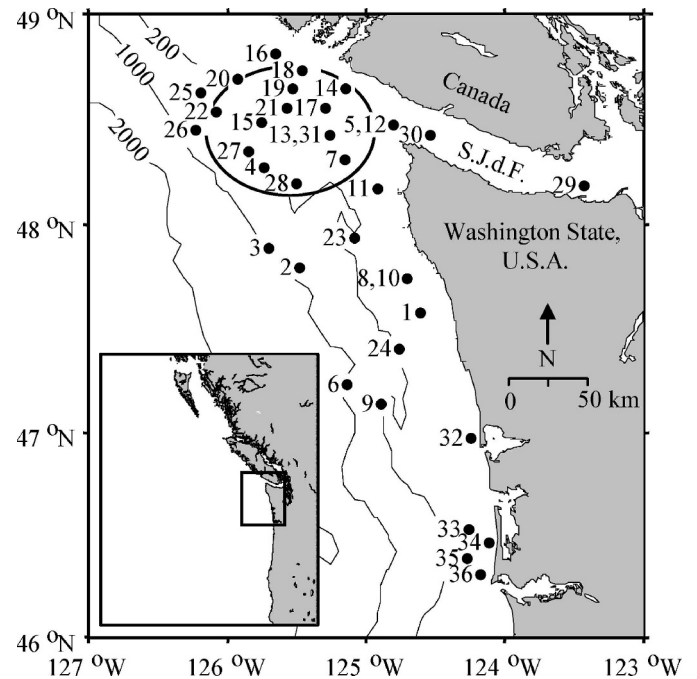


Fig. 1. Location of experimental stations on the coast of the Pacific Northwest used for the 36 *P-n* spp. and size-fractionated Chl *a* growth and grazing experiments. Depth contours are shown. Large open circle shows the approximate location of the Juan de Fuca eddy. S.J.d.F., Strait of Juan de Fuca.

during four ECOHAB-PNW cruises in 2003 (30 Aug–19 Sep), 2004 (08–28 Sep), and 2005 (07–27 Jun, and 02–22 Sep) on the PNW continental shelf (Fig. 1). Experimental stations were spatially widespread and encompassed the dominant physical-chemical regimes in the area: the coastal upwelling zone, the Juan de Fuca eddy, and the offshore zone. Temperature and salinity data on all four cruises were collected using a Sea-Bird Electronics SBE 911 plus conductivity, temperature, and depth (CTD) system with dual temperature and conductivity sensors mounted on a rosette equipped with 10-liter Niskin bottles. Thirty-six growth and grazing experiments were conducted at locations where *P-n* spp. were present. These experiments were performed across diverse chemical, physical (Table 1), and biological (Table 2) conditions.

*Growth and grazing experiments*—Estimates of specific growth rate ( $\mu$ ,  $d^{-1}$ ) and specific microzooplankton grazing ( $g$ ,  $d^{-1}$ ) of both *P-n* spp. and the size-fractionated Chl *a* ( $<5 \mu m$  and  $>5 \mu m$ ) were determined simultaneously using the seawater-dilution technique (e.g., Landry et al. 1995). Seawater was collected from the depth corresponding to 50% surface irradiance, which was usually between 3- and 5-m depth. This depth was chosen because it typically corresponded to the depth of maximum *P-n* abundance. Particle-free diluent water (PFW) was made by first pooling the water from several Niskin bottles into a 50-liter polyethylene carboy and then gravity filtering this water through an in-line cascade of 3- $\mu m$  and 0.2- $\mu m$  Pall Gelman pleated capsule filters into a 20-liter polycarbonate carboy. Experimental bottles (2.5-liter polycarbonate bottles) were

Table 1. Initial environmental conditions of seawater collected for growth and grazing experiments in the Pacific Northwest during 2003, 2004, and 2005. Temperature values in parenthesis are the 24-h average of 5-min averaged data from within the experimental incubators and are the values used in the MLR analysis. PAR values are expressed as 50% of surface values. C, coastal; MS, midshelf; OS, offshore; JDE, Juan de Fuca eddy; ISJF, Inner Strait of Juan de Fuca; SJFO, Strait of Juan de Fuca outflow; VICC, Vancouver Island Coastal Current; UW, upwelling; DW, downwelling; SDW, strong downwelling; BM, bloom. Italicized values are averages for each cruise. ND, no data. Nitrate values <0.1 are below detection limit.

Exp.	Date	Latitude (N)	Longitude (W)	Location description	Temp (°C)	Salinity	PAR (mol quanta m <sup>-2</sup> 24 h <sup>-1</sup> )	Nutrients (μmol L <sup>-1</sup> )		
								Nitrate	Phosphate	Silicic acid
1	01 Sep 03	47°52.78	124°64.15	C, UW	10.0 (11.5)	32.8	79.0	18.4	1.31	36.0
2	03 Sep 03	47°88.30	125°53.37	OS	13.3 (14.9)	32.0	72.8	1.1	0.37	11.9
3	06 Sep 06	47°98.35	125°72.32	OS	13.9 (15.4)	31.7	27.2	4.0	0.50	26.0
4	09 Sep 06	48°26.17	125°66.72	JDE	13.4 (14.9)	31.6	49.2	9.2	0.87	29.6
5	12 Sep 03	48°43.75	124°85.57	SJFO	11.0 (12.5)	32.5	69.0	6.1	0.57	25.7
6	14 Sep 03	47°25.95	125°06.13	OS	15.0 (16.5)	31.9	65.2	0.7	0.37	6.0
7	16 Sep 03	48°32.25	125°06.85	JDE	11.9 (13.4)	32.2	52.6	14.1	1.28	32.3
					<i>12.6 (14.2)</i>	<i>32.1</i>	<i>59.3</i>	<i>7.7</i>	<i>0.80</i>	<i>23.9</i>
8	09 Sep 04	47°76.83	124°80.50	C, DW	14.6 (17.5)	32.2	31.6	0.8	0.25	13.0
9	10 Sep 04	47°16.80	124°88.25	MS, SDW	16.5 (16.4)	32.1	25.8	<0.1	0.18	6.3
10	11 Sep 04	47°76.88	124°80.55	C, SDW	13.2 (15.6)	32.2	27.0	4.9	0.44	16.0
11	12 Sep 04	48°21.73	124°87.15	C, DW, BM	13.8 (14.1)	32.3	18.2	1.6	0.25	18.6
12	13 Sep 04	48°43.75	124°85.43	C, BM	12.6 (13.8)	32.2	11.0	6.3	0.59	25.7
13	14 Sep 04	48°32.87	125°33.95	JDE, BM	12.9 (13.8)	32.3	8.6	9.7	0.74	25.9
14	14 Sep 04	48°57.48	125°16.68	JDE	11.8 (14.3)	31.8	25.2	15.4	1.27	38.9
15	15 Sep 04	48°47.60	125°75.50	JDE	12.7 (13.2)	32.4	21.0	7.8	0.60	25.5
16	16 Sep 04	48°78.23	125°57.17	VICC, SJFO	11.8 (13.3)	31.5	18.4	18.3	1.52	42.4
17	17 Sep 04	48°53.93	125°25.60	JDE, BM	13.3 (13.4)	32.3	28.0	7.6	0.67	21.8
18	18 Sep 04	48°68.62	125°48.37	JDE, BM	12.7 (13.5)	32.2	33.2	8.0	0.70	23.0
19	18 Sep 04	48°56.77	125°54.35	JDE, BM	12.7 (13.5)	32.3	33.0	3.0	0.41	26.8
20	19 Sep 04	48°66.83	125°84.65	JDE, BM	12.4 (13.8)	32.3	28.2	5.4	0.54	25.8
21	20 Sep 04	48°46.72	125°66.80	JDE, BM	12.8 (14.5)	32.3	32.4	4.3	0.47	27.0
22	21 Sep 04	48°53.02	126°02.63	JDE, BM	13.6 (14.1)	32.3	15.6	1.9	0.32	23.3
23	22 Sep 04	47°93.67	125°00.29	MS, DW	14.4 (15.9)	32.1	8.8	0.1	0.12	9.7
24	22 Sep 04	47°47.82	124°78.25	MS, DW	14.5 (15.9)	32.0	25.0	<0.1	0.09	11.2
25	23 Sep 04	48°56.73	126°08.32	JDE, BM	13.9 (14.8)	32.2	28.4	1.9	0.34	15.3
26	24 Sep 04	48°49.33	126°08.12	JDE, BM	14.0 (14.6)	32.2	30.2	2.5	0.40	18.0
27	25 Sep 04	48°35.53	125°83.18	JDE, BM	14.2 (15.4)	32.1	21.6	<0.1	0.34	16.9
28	26 Sep 04	48°15.40	125°53.68	JDE, BM	14.2 (16.2)	32.1	27.0	<0.1	0.28	14.4
					<i>13.4 (14.6)</i>	<i>32.2</i>	<i>23.7</i>	<i>4.7</i>	<i>0.5</i>	<i>21.2</i>
29	15 Jul 05	48°14.00	125°43.00	ISJF	11.2 (12.8)	31.2	20.8	17.5	ND	33.0
30	21 Jul 05	48°40.35	124°59.38	VICC	12.8 (14.3)	31.7	18.2	7.0	ND	25.3
31	22 Jul 05	48°36.20	125°30.27	JDE	11.5 (15.4)	31.2	20.6	14.8	ND	30.5
					<i>11.8 (14.2)</i>	<i>31.4</i>	<i>19.9</i>	<i>13.1</i>		<i>29.6</i>
32	08 Sep 05	47°04.06	124°14.74	C, UW	11.0 (16.6)	33.1	19.4	15.2	ND	33.6
33	09 Sep 05	46°50.45	124°22.02	C, UW	13.7 (13.3)	32.8	13.4	2.9	ND	8.4
34	10 Sep 05	46°39.95	124°13.50	C, UW	10.1 (13.6)	33.0	11.6	18.0	ND	33.3
35	11 Sep 05	46°31.21	124°16.34	C, DW	13.0 (13.7)	32.8	12.2	4.4	ND	16.6
36	12 Sep 05	46°31.76	124°10.91	C, DW	11.4 (13.7)	32.9	11.6	9.0	ND	7.5
					<i>11.9 (14.2)</i>	<i>32.9</i>	<i>13.6</i>	<i>9.9</i>		<i>19.9</i>

filled to predetermined levels with this PFW. All containers, tubing, and in-line filters were acid-cleaned prior to use with 5% (v/v) HCl acid and rinsed copiously with deionized water. Clean techniques were used throughout all experimental and sample manipulation.

Whole seawater (WSW) was drained from several Niskin bottles (same cast as PFW) using silicone tubing with end caps of 200-μm mesh into a 50-liter polyethylene carboy. Although delicate microzooplankton may be damaged by this filtering process, it was necessary to remove abundant mesozooplankton. Care was taken to minimize damage,

and qualitative assessment revealed no discernible difference between prescreened and unscreened water. The WSW was kept well-mixed by gentle stirring with a polyethylene plunger. The WSW was siphoned from the 50-liter WSW carboy into the experimental bottles containing the PFW to reach either five (0.1, 0.2, 0.4, 0.7, and 1.0 WSW; experiments 1–7) or three (0.1, 0.5, and 1.0 WSW; experiments 8–36) target dilution levels. Experimental bottles were amended with nutrients to achieve enrichments of 10 μmol L<sup>-1</sup> nitrate (NaNO<sub>3</sub>), 0.63 μmol L<sup>-1</sup> phosphate (NaH<sub>2</sub>PO<sub>4</sub>·H<sub>2</sub>O), 10 μmol L<sup>-1</sup> silicic acid (Na<sub>2</sub>O<sub>3</sub>Si·

Table 2. Initial size-fractionated Chl *a*, *P-n* spp., and domoic acid concentrations for each growth and grazing experiment. ND, no data available. The percentage contribution of *P-n* spp. biomass to total phytoplankton biomass was calculated as described in methods section. *P-n*, *Pseudo-nitzschia* spp.; C, carbon.

Exp	Chl <i>a</i> ( $\mu\text{g L}^{-1}$ )			<i>P-n</i> spp. abundance (cells $\text{L}^{-1}$ )			% contribution <i>P-n</i> Chl <i>a</i> to total Chl <i>a</i>	Domoic acid		
	<5 $\mu\text{m}$	>5 $\mu\text{m}$	Total	Small ( $\times 10^5$ )	Large ( $\times 10^5$ )	Total ( $\times 10^5$ )		pDA ( $\text{ng L}^{-1}$ )	pDA ( $\text{ng } \mu\text{g}^{-1}$ <i>P-n</i> C)	dDA ( $\text{nmol L}^{-1}$ )
1	0.6	10.1	10.7	2.63	0.49	3.13	1.3	<0.001	<0.001	ND
2	0.9	8.9	9.8	1.09	0.19	1.28	0.6	40	12.6	ND
3	2.8	13.4	16.3	0.76	0.18	0.94	0.3	378	140.0	ND
4	1.8	3.3	5.0	0.47	0.06	0.53	0.4	93	81.7	ND
5	0.6	21.3	21.9	2.81	0.40	3.21	0.6	56	7.7	ND
6	0.4	0.6	1.0	0.05	0.19	0.24	3.6	2,014	993.4	ND
7	1.1	1.5	2.5	0.16	0.13	0.29	1.1	ND	ND	ND
8	2.3	2.9	5.2	7.69	0.90	8.59	6.1	342	19.2	0.3
9	0.5	0.3	0.8	0.80	0.02	0.82	2.3	34	31.4	3.8
10	1.1	2.1	3.2	5.36	0.45	5.81	5.9	236	22.4	4.7
11	3.3	6.1	9.4	13.43	0.22	13.65	3.2	1,461	113.2	5.0
12	3.0	5.9	9.0	18.04	0.08	18.12	4.1	1,586	77.0	1.4
13	ND	ND	ND	18.32	0.03	18.35	ND	2,705	132.7	0.5
14	ND	ND	ND	6.16	0.00	6.16	ND	1,057	156.6	2.1
15	1.3	0.8	2.0	4.99	0.08	5.07	5.6	684	108.6	1.1
16	1.0	0.7	1.8	2.81	0.00	2.81	3.0	187	60.7	0.6
17	1.2	4.1	5.3	28.79	0.00	28.79	10.6	2,767	87.7	1.9
18	1.9	3.7	5.6	24.59	0.23	24.82	9.3	2,301	78.4	2.8
19	4.7	11.1	15.8	40.83	0.00	40.83	5.1	3,265	73.0	4.1
20	ND	ND	ND	31.17	0.11	31.28	ND	3,265	92.5	1.6
21	3.9	6.1	10.0	25.79	0.14	25.93	5.3	3,390	114.1	2.2
22	4.1	7.7	11.7	49.30	0.56	49.86	9.1	7,744	129.4	5.5
23	1.9	6.0	7.9	68.78	0.20	68.98	17.5	6,096	78.7	5.0
24	1.7	4.0	5.7	23.62	0.00	23.62	8.1	5,318	205.4	1.4
25	2.3	6.3	8.5	64.20	0.39	64.59	15.6	11,009	147.9	15.3
26	1.1	1.9	2.9	19.05	0.30	19.35	14.7	1,810	75.4	17.7
27	4.3	4.1	8.4	10.61	0.00	10.61	2.5	995	85.6	1.9
28	2.8	2.8	5.6	34.61	0.06	34.67	12.3	5,163	134.0	1.4
29	0.6	6.7	7.3	0.02	0.28	0.30	0.7	271	92.5	0.0
30	0.9	15.0	15.9	0.78	0.15	0.94	0.3	46	19.1	0.9
31	1.2	7.6	8.8	0.57	0.05	0.63	0.2	65	56.9	ND
32	0.6	5.6	6.3	0.24	0.07	0.32	0.3	ND	ND	ND
33	1.9	7.3	9.1	2.48	0.08	2.56	0.7	180	50.7	0.7
34	0.9	5.7	6.5	0.53	0.04	0.57	0.3	12	12.0	2.0
35	2.6	14.2	16.8	2.05	0.15	2.20	0.4	339	89.1	1.4
36	2.7	15.1	17.8	2.28	0.18	2.46	0.4	267	61.1	3.5

9H<sub>2</sub>O), and 3 nmol L<sup>-1</sup> Fe (Fe in 2% HCl) to the ambient water concentrations. An additional set of 1.0 WSW bottles was used without nutrient amendments to test for potential nutrient limitation of *P-n* spp. and the phytoplankton communities. Duplicate samples were randomly taken from the WSW carboy during water disbursement for microscopy, nutrients, and DA analysis.

Dilution treatment bottles were placed in clear Plexiglas tubes covered with Mylar film to simulate the in situ irradiance. The tubes were secured to a revolving wheel (1 rpm) submerged in a Plexiglas on-deck incubator and incubated for 24 h. The temperature inside the incubator was maintained near in situ levels using continuously flowing surface seawater. Incident photosynthetically active radiation (PAR) was measured with a Hobo Par Smart Sensor and data logger mounted on the incubator, and water temperature was monitored inside the incubator with

a submerged Hobo Water Temp Pro data logger. PAR ( $\mu\text{mol quanta m}^{-2} \text{s}^{-1}$ ), recorded in 2 min averages, was summed as  $\text{s}^{-1}$  values over 24 h and multiplied by 0.5 to estimate irradiance experienced in the incubation bottles; these values are expressed as  $\text{mol quanta m}^{-2} 24 \text{ h}^{-1}$ . Temperature values were recorded every 5 min and were averaged over 24 h.

In each replicate dilution bottle, the nutrient-amended net growth rate ( $k_n$ ) was determined according to  $k_n = \ln(N_1/N_0)/(t_1 - t_0)$ , where  $N_1$  and  $N_0$  are the final *P-n* spp. or size-fractionated Chl *a* concentration at time 1 ( $t_1$ ) and time 0 ( $t_0$ ), respectively. The intrinsic rates of growth ( $\mu$ ,  $\text{d}^{-1}$ ) and mortality due to grazing by microzooplankton ( $g$ ,  $\text{d}^{-1}$ ) of *P-n* spp. and the size-fractionated Chl *a* were calculated by linear regression of net growth rate ( $k_n$ ) in each nutrient-amended dilution bottle against the fraction of WSW,  $D_i$ . *P-n* spp.- or Chl *a*-based growth ( $\mu$ ) was determined by

extrapolation of the regression to the ordinal intercept, where  $D_i$  (proportional to grazing mortality,  $g$ ; Landry et al. 1995) becomes zero, and so,  $k_n = \mu_n$ . Because nutrients were added to our treatment bottles, if phytoplankton growth is limited by in situ nutrient concentrations,  $\mu_n$  as calculated here is a *potential* growth rate. When nutrient-limited growth was observed in the 1.0 WSW control bottles, the in situ intrinsic rate ( $\mu_{un}$ ), was estimated from  $\mu_{un} = k_{un1.0} + g$ , where  $k_{un1.0}$  is the net growth rate in the 1.0 WSW treatment without added nutrients (Landry et al. 1995). Microzooplankton grazing rates on *P-n* spp. and the Chl *a* size fractions were determined by the slope of linear regressions of  $k_n$  and  $D_i$ . On two occasions, dilution regressions showed evidence (nonlinearity) of saturated grazing kinetics (Gallegos 1989). For these experiments,  $\mu$  was calculated using the linear portion of the regression, while  $g$  was calculated using  $g = \mu_n - k_{n1.0}$ , where  $k_{n1.0}$  is the net growth rate in the nutrient-enhanced 1.0 WSW dilution treatment. If differential net growth of microzooplankton occurred across dilution levels, these estimates will be biased (Landry et al. 1995, Dolan and McKeon 2004; Landry and Calbet 2004). Assessing and correcting for this potential bias, however, is not straightforward (e.g., identifying which taxa are the relevant herbivores). Moreover, recent evidence suggests that microzooplankton growth rates in experiments in diverse coastal environments show no consistent pattern across dilutions, and adjustments for microzooplankton growth do not significantly change estimates of  $\mu$  and  $g$  (First et al. 2007). Therefore, corrections for microzooplankton growth were not made in this study.

**Sample processing**—Initial samples were taken from the WSW carboy and final samples were taken from dilution treatment bottles for microscopy, Chl *a*, nutrients, and particulate DA (pDA) and dissolved DA (dDA) analyses. Samples were taken in quadruplicate for initial size-fractionated Chl *a* analysis and in duplicate from each treatment bottle for final size-fractionated Chl *a* analysis. For microscopy, duplicate 250-mL samples were preserved with both acid Lugol's solution (final concentration 5%) and glutaraldehyde (final concentration of 0.5%). Within hours of sampling, aliquots of the glutaraldehyde-fixed samples were stained with 4'-6-diamidino-2-phenylindole (DAPI) and proflavin and filtered onto 0.2- $\mu$ m (for nanoplankton; volumes filtered = 10 to 30 mL) and 0.8- $\mu$ m (for microplankton <40  $\mu$ m; volumes filtered = 50 to 150 mL) black polycarbonate GE Osmonics filters overlaying 1.2- $\mu$ m cellulose backing filters (Lessard and Murrell 1996). The filters were mounted on slides using Resolve microscope immersion oil, and the exposed edges were sealed with paraffin. Slides were stored in a  $-20^\circ\text{C}$  freezer for microscopic analysis onshore.

**Pseudo-nitzschia counts and biomass estimates**—*P-n* spp. were counted and sized on the glutaraldehyde-fixed samples using a Zeiss epifluorescent microscope at  $\times 400$  magnification. *P-n* spp. were separated into two size categories, small and large, based upon the width of the cell valve. *P-n* spp. with a transapical axis narrower than

3  $\mu$ m were categorized as small cells; this grouping included the species *P. pseudodelicatissima*, *P. delicatissima*, and *P. cuspidata*. Cells with a transapical axis wider than 3  $\mu$ m were considered large cells; this grouping included the species *P. australis*, *P. fraudulentheimii*, *P. pungens*, and *P. multiseriis* (Horner 2002). To calculate the contribution of *P-n* spp. Chl *a* to total Chl *a*, *P-n* spp. cellular carbon was estimated by first calculating *P-n* spp. biovolume using diamond-shaped box geometry  $V = (L \times W^2)/2$ , where  $V$  is volume ( $\mu\text{m}^3$ ),  $L$  is the maximum length, and  $W$  is the maximum transapical width of the cell. *P-n* spp. biovolume was converted into cellular C using the diatom equation of Menden-Deuer and Lessard (2000). Approximately 1,000 each of small and large *P-n* spp. cells in randomly selected samples from several experiments were measured once for biomass estimations. The average cell biomass was 10.96 pg C cell $^{-1}$  and 103.82 pg C cell $^{-1}$  for small and large cells, respectively. To estimate the Chl *a* contribution of *P-n* spp. to the aggregate Chl *a* biomass in each experiment, *P-n* spp. biomass was divided by a C:Chl *a* ratio of 56 (Marchetti and Harrison 2007).

**Microzooplankton abundance and biomass**—Heterotrophic nanoflagellates and small heterotrophic dinoflagellates (<40  $\mu$ m) were counted with epifluorescent microscopy on 0.2- $\mu$ m filters and 0.8- $\mu$ m filters at  $\times 1000$  and  $\times 400$  magnification, respectively. Ciliates, large heterotrophic dinoflagellates (>40  $\mu$ m), and the mixo-autotrophic dinoflagellates *Ceratium* and *Prorocentrum* spp. were counted and sized in settled Lugol's-preserved samples with an inverted Zeiss microscope at  $\times 250$  using a computer-aided digitizing system (Roff and Hopcroft 1986). No fewer than 400 cells were counted and measured for each sample. Cell volumes were calculated using appropriate geometric formulas, and carbon was estimated from the equations in Menden-Deuer and Lessard (2000) and Putt and Stoecker (1989) for flagellates and ciliates, respectively.

**Chlorophyll**—Samples for size-fractionated Chl *a* analysis were stored in a cooler during experimental setup. Within 15 min, these samples were filtered through an in-line fractionation cascade consisting of 45-mm-diameter GE Osmonics polycarbonate (pore size = 5.0  $\mu$ m) and 25-mm-diameter Whatman GF/F (nominal pore size = 0.7  $\mu$ m) filters. Filters were extracted in 90% acetone for 24 h at  $-20^\circ\text{C}$ , and fluorescence was measured with a Turner Designs 10AU fluorometer using either the acidification method of Parsons et al. (1984) for 2003 samples, or the nonacidification method of Welschmeyer (1994) for the 2004 and 2005 samples. Chl *a* samples for experiments 13, 14, and 20 were lost and are excluded from analysis. The fluorometer used at sea was calibrated at the beginning of each cruise with pure Chl *a* standards (Turner Designs).

**Nutrients**—Unfiltered duplicate samples for nutrient analysis were collected in precleaned polypropylene tubes (BD Falcon) during the experimental setup from the 50-liter WSW carboy and were either kept dark and refrigerated ( $4^\circ\text{C}$ ) and run within 1–2 days shipboard, or

frozen at  $-20^{\circ}\text{C}$  for later analysis. In either case, samples were brought to room temperature and analyzed with a Lachat QuickChem 8000 Flow Injection Analysis system using standard colorimetric techniques for the concentration of nitrate + nitrite (hereafter referred to as nitrate; Smith and Bogren 2001), orthophosphate (Knepel and Bogren 2002), and silicic acid (Wolters 2002).

**Domoic acid**—For pDA, 1 liter of seawater was filtered through a 47-mm-diameter Millipore nitrocellulose filter (pore size =  $0.45\ \mu\text{m}$ ). Upon filtration, the filter was placed in a centrifuge tube (BD Falcon) containing 4 mL of nanopure water kept near freezing until analysis. For dDA,  $\sim 1\ \text{mL}$  of  $0.45\text{-}\mu\text{m}$ -filtered seawater was placed in a cryovial and frozen at  $-80^{\circ}\text{C}$  until analysis. Concentrations of pDA and dDA were analyzed using the receptor binding assay (Van Dolah et al. 1997; Trainer et al. 2002) or indirect competitive Enzyme Linked ImmunoSorbent Assay (cELISA). For dDA analysis using cELISA, samples were diluted  $25\times$  with distilled water to remove seawater matrix effects and analyzed using Biosense direct cELISA kits (Biosense Laboratories). All samples were run in triplicate, and sample DA concentrations were interpolated from a certified DA standard curve (DACS-1B, National Research Council, Canada). The uncorrected working range of this assay was  $5\text{--}83\ \text{pg DA mL}^{-1}$ ; therefore, the limit of quantification was  $\sim 5\ \text{pg DA mL}^{-1}$ , and limit of detection was  $\sim 1\ \text{pg DA mL}^{-1}$ . Assay precision was coefficient of variation (CV)  $<20\%$  for the cELISA and  $5\%$  for the receptor binding assay. Total pDA was normalized to *P-n* spp. cell biomass to give an approximate index of cellular toxicity.

**Statistical tests and multiple linear regression**—A one-way analysis of variance (ANOVA) was used to assess differences in hydrographic data across years. The exception was the analysis of PAR because the assumption of equal variance was not met, so these data were analyzed with a Kruskal–Wallis one-way ANOVA. Differences in *P-n* spp. intrinsic growth ( $\mu$ ) and grazing ( $g$ ) across years were non-normally distributed, and thus they were tested using a Kruskal–Wallis one-way ANOVA. Due to non-normal distributions, comparisons between *P-n* and Chl *a*-specific grazing rates were made using Kruskal–Wallis one-way ANOVA. All correlations were made using the Pearson Product Moment test. All data were analyzed using SigmaStat 3.0 or SPSS statistical software.

In order to determine the simultaneous environmental variables that most influence the intrinsic growth rates of *P-n* spp. and the size-fractionated Chl *a*, we used a forward multiple stepwise regression analysis (MLR) (Neter et al. 1996). In our model, intrinsic growth of *P-n* spp. and the size-fractionated Chl *a* were regressed against several independent environmental explanatory variables. Forward multiple stepwise regression develops a sequence of regression models, and at each step, an explanatory variable is added or dropped, depending on predetermined criteria. In this study, the critical value for an explanatory variable to enter or exit our model was set at  $p = 0.050$  and  $p = 0.100$ , respectively. The stepwise

procedure ends with the identification of the single best regression model containing  $x + \dots + n$  explanatory variables. For the two independent variables, temperature and PAR, we used the averaged values over the 24-h incubation rather than the in situ values at time of experimental water collection.

## Results

**Environmental conditions**—The hydrographic conditions and macronutrient concentrations at our experimental stations varied greatly on short time and space scales (Table 1), highlighting the dynamic nature of this temperate upwelling coastal environment. The most conspicuous example of this variability is the range of macronutrient concentrations observed during this study; at our experimental stations, the surface concentrations of nitrate and silicic acid ranged from below detection ( $<0.1\ \mu\text{mol L}^{-1}$ ) to  $18.4\ \mu\text{mol L}^{-1}$  and  $6.0$  to  $36.4\ \mu\text{mol L}^{-1}$ , respectively. Salinity at our experimental stations ranged from 31.2 to 33.1. Highest salinity values were seen in Sep 2005 during an upwelling event. In situ water temperatures ranged from  $10^{\circ}\text{C}$  to  $16.5^{\circ}\text{C}$ ; temperatures during incubations were on average  $1.5^{\circ}\text{C}$  higher than in situ collection temperature. PAR levels across years were significantly different ( $p < 0.001$ ), and levels in 2003 were significantly higher than 2004 and 2005 (Table 1).

**Pseudo-nitzschia spp. distribution, abundance, and DA**—*P-n* spp. abundance was variable in both time and space at our experimental stations, ranging from  $2.4 \times 10^4\ \text{cells L}^{-1}$  to  $>6.0 \times 10^6\ \text{cells L}^{-1}$  (Table 2). Maximum *P-n* spp. abundance was found during a Juan de Fuca eddy bloom in Sep 2004 (Fig. 1; Table 2). This bloom was codominated by *P. cf. cuspidata* and the euglenoid *Eutreptiella* sp. Overall, the small morphotypes *P. cuspidata*, *P. pseudodelicatissima*, and *P. delicatissima* dominated *P-n* spp. abundance across the study region in time and space. When present, the large *P-n* spp. were represented by *P. australis*, *P. fraudulenta*, *P. heimii*, *P. multiseries*, and *P. pungens* (V. L. Trainer pers. comm.).

Generally, *P-n* spp. contributed very little to total phytoplankton Chl *a* (avg.  $4.6\%$ ,  $n = 33$ ) (Table 2). The contribution of *P. cf. cuspidata* to total Chl *a* within the Juan de Fuca eddy bloom in Sep 2004 was higher, but even then, the average contribution to the total phytoplankton Chl *a* was only  $8.4\%$  ( $n = 11$ , range  $3.2\text{--}15.6\%$ ; Table 2).

The highest total pDA concentrations were seen in the 2004 Juan de Fuca eddy bloom, when the maximum concentration exceeded  $11\ \mu\text{g pDA L}^{-1}$  (Table 2). These high pDA concentrations were mostly a result of high *P-n* spp. cell abundance; when pDA is normalized to *P-n* carbon content, concentrations of pDA were, on average, greater in 2004 ( $87.7\ \text{ng pDA} [\mu\text{g } P\text{-n C}]^{-1}$ ) than in 2003 ( $47.2\ \text{ng pDA}$ ) and 2005 ( $56.9\ \text{ng pDA}$ ), but values were not statistically different between years (Kruskal–Wallis one-way ANOVA on ranks,  $p > 0.05$ ). The highest dDA values were found within the Juan de Fuca eddy bloom, and maximum dDA values reached  $>17\ \text{nmol L}^{-1}$  (Table 2).

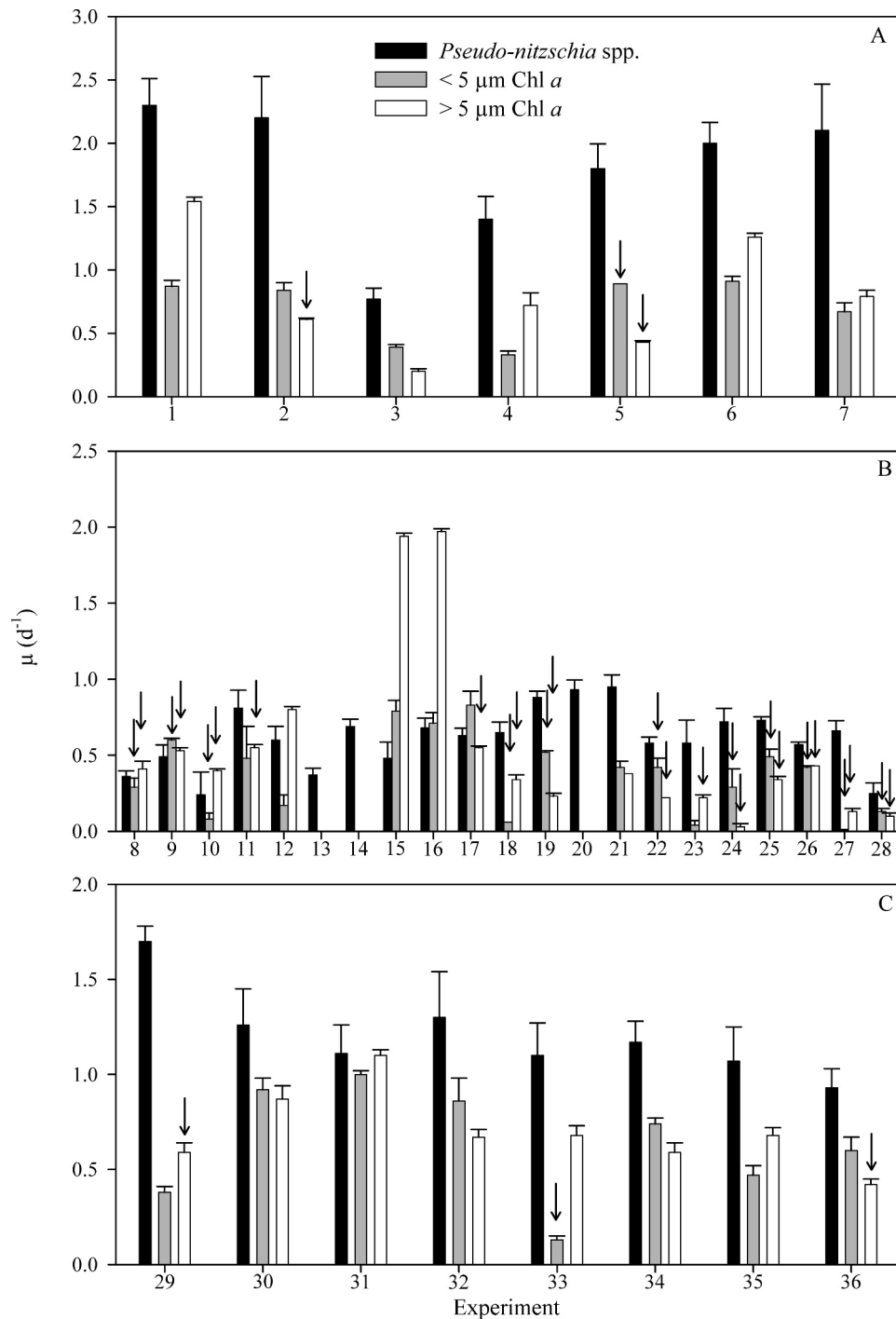


Fig. 2. Intrinsic growth rates ( $\mu$ ,  $d^{-1}$ ) of *P-n* spp.,  $< 5 \mu m$  Chl *a*, and  $> 5 \mu m$  Chl *a* for (A) Sep 2003 (exp. 1–7), (B) Sep 2004 (exp. 8–28), and (C) Jul (exp. 29–31) and Sep (exp. 32–36) 2005. Error bars are the standard error of the ordinal intercept from dilution linear regressions. Arrows indicate experiments and size fractions where nutrient-enhanced growth rates were observed. Intrinsic growth rates shown are corrected for nutrient enhancement as described in methods section. Note the change in scale of the ordinal axis for each plot.

*Pseudo-nitzschia* spp. and Chl *a* intrinsic growth rates—*P-n* spp. intrinsic growth rates ranged from  $0.24 d^{-1}$  to  $2.30 d^{-1}$  (Fig. 2). Highest *P-n* spp. intrinsic growth rates were seen in 2003, with maximum rates  $> 2.00 d^{-1}$  on several occasions (Fig. 2; Table 3). The lowest intrinsic

growth rates were observed in 2004, when maximum *P-n* spp. abundance was observed, and rates were significantly lower than 2003 and pooled Jul and Sep 2005 rates (Kruskal–Wallis ANOVA,  $p < 0.001$ ). The average *P-n* spp. growth rate across years, and across wide-ranging

Table 3. Average *P-n* spp. and size-fractionated Chl *a* intrinsic growth ( $\mu$ , d<sup>-1</sup>) and grazing rates for 2003, 2004, and 2005. The ranges of values are shown in parentheses. The average growth and grazing rates for *P-n* and the Chl *a* size fractions were calculated from an *n* of 36 and 33, respectively.

Year	Growth ( $\mu$ , d <sup>-1</sup> )			Grazing (g, d <sup>-1</sup> )		
	<i>P-n</i>	Chl <i>a</i>		<i>P-n</i>	Chl <i>a</i>	
		<5 $\mu$ m	>5 $\mu$ m		<5 $\mu$ m	>5 $\mu$ m
2003						
September ( <i>n</i> =7)	1.80 (0.77–2.30)	0.70 (0.33–0.91)	0.79 (0.20–1.54)	0.95 (0.03–1.70)	0.60 (0.23–0.87)	0.31 (0.01–0.53)
2004						
September ( <i>n</i> =21)	0.61 (0.24–0.95)	0.37 (0.01–0.83)	0.53 (0.03–1.97)	0.22 (0.03–0.52)	0.46 (0.13–1.24)	0.17 (0.00–0.53)
2005						
July ( <i>n</i> =3)	1.36 (1.11–1.70)	0.77 (0.38–1.00)	0.85 (0.59–1.10)	0.14 (0.04–0.20)	0.62 (0.37–0.76)	0.19 (0.05–0.27)
September ( <i>n</i> =5)	1.12 (0.93–1.30)	0.56 (0.13–0.86)	0.61 (0.42–0.68)	0.11 (0.00–0.28)	0.35 (0.21–0.60)	0.21 (0.03–0.37)
Average ( <i>n</i> =36, 33)	0.97	0.50	0.62	0.32	0.49	0.21

macronutrient and hydrographic conditions, was relatively high at 0.97 d<sup>-1</sup> (Table 3). We did not find any evidence of nutrient limitation in *P-n* spp. (Fig. 2); net growth rates in 1.0 WSW dilution treatments with and without nutrient amendments were statistically the same in all cases, even when macronutrients were found at concentrations normally considered limiting for diatom growth.

Although *P-n* spp. contributed to the aggregate Chl *a*, this contribution was minimal (4.6% on average); as such, for our comparisons, we treated the Chl *a*-based and *P-n* spp.-based growth and grazing rates independently. *P-n* spp. growth rates were consistently higher than the corresponding intrinsic growth rates of the <5- $\mu$ m and >5- $\mu$ m aggregate Chl *a* by an average factor of 1.9 and 1.6, respectively (Fig. 2; Table 3). There were only a few occasions when any Chl *a* size fraction grew faster than *P-n* spp. (Fig. 2). On average, the >5- $\mu$ m Chl *a* size fraction had higher intrinsic growth rates ( $\bar{x}$  = 0.62 d<sup>-1</sup>) than the

<5- $\mu$ m Chl *a* size fraction ( $\bar{x}$  = 0.50 d<sup>-1</sup>; Table 3), but the number of locations where >5- $\mu$ m Chl *a* size fraction grew faster than the <5- $\mu$ m Chl *a* size fraction was equal to the number of locations where the larger fraction grew slower than the smaller cell-sized fraction. Both the <5- $\mu$ m and >5- $\mu$ m Chl *a* size fractions, unlike *P-n* spp., showed signs of nutrient-limited growth (Fig. 2), even during conditions of moderate to elevated macronutrient concentrations (Table 1). Generally, when nutrient-stressed, both the <5- $\mu$ m and >5- $\mu$ m Chl *a* size fractions showed growth responses to added nutrients; this was especially evident during Sep 2004 (Fig. 2B). There was only one instance (Sep 2005) when the <5- $\mu$ m Chl *a* size fraction demonstrated a stress response unaccompanied by a corresponding response in the >5- $\mu$ m Chl *a* size fraction, whereas stress in the >5- $\mu$ m Chl *a* size fraction unaccompanied by a response in the <5- $\mu$ m Chl *a* size fraction was frequently observed (six experiments).

Table 4. Results of multiple stepwise regression analysis of *P-n* spp., <5- $\mu$ m Chl *a*, and >5- $\mu$ m Chl *a* size fraction intrinsic growth rate ( $\mu$ , d<sup>-1</sup>). In all analyses, light, temperature, salinity, nitrate, silicic acid, and pDA were included as potential predictors of intrinsic growth. Temperature data used in the analysis are the average 24-h temperatures within the experimental incubators; *p* values of significant and nonsignificant predictors of intrinsic growth are given for each analysis. Temp, temperature; Sal, salinity; N, nitrate; Si, silicic acid; pDA, particulate domoic acid.

Dependent variable	Included predictors ( <i>p</i> )	Excluded predictors ( <i>p</i> )	Adj. <i>r</i> <sup>2</sup>	SE	<i>n</i>	$Y = \beta_0 + \beta_1 X_1 + \dots + \beta_n X_n$
<i>Pseudo-nitzschia</i> $\mu$	light (<0.000) temp (0.003)	Sal (0.299) N (0.345) Si (0.531) pDA (0.221)	0.61	0.33	36	$Y = 2.499 + 0.033(\text{light}) - 0.144(\text{temp})$
<5- $\mu$ m Chl <i>a</i> $\mu$	N (0.006) light (0.020)	Sal (0.737) temp (0.696) Si (0.874)	0.29	0.25	33	$Y = 0.196 + 0.220(N) + 0.005(\text{light})$
>5- $\mu$ m Chl <i>a</i> $\mu$	N (0.001)	Sal (0.489) temp (0.400) light (0.283) Si (0.457)	0.29	0.40	33	$Y = 0.350 + 0.043(N)$

**Multiple linear regression results**—The results of our multiple regression analysis demonstrate that the intrinsic growth of *P-n* spp. is significantly predicted by light and temperature (adj.  $r^2 = 0.61$ ; Table 4). The correlation with temperature (24-h average within incubators) was negative, and no collinearity was seen with temperature, nitrate, or salinity, indicating that higher growth at low temperatures was not associated with the colder, more saline, and nutrient-rich recently upwelled water. However, we were concerned that the lack of collinearity between these seemingly, especially in upwelling environments, related variables was a result of the incubator temperatures being variable and, on average, slightly higher than the in situ water temperature. As such, we also ran the model using in situ water temperatures (data not shown) from time of water collection and, again, saw no collinearity between nitrate and temperature. *P-n* spp. growth was not predicted by the ambient concentrations of silicic acid, pDA or, surprisingly, nitrate. This is in contrast to the  $<5\text{-}\mu\text{m}$  and  $>5\text{-}\mu\text{m}$  Chl *a* size fractions, both of which showed dependence on initial nitrate concentrations, but not silicic acid. Similar to *P-n* spp., the  $<5\text{-}\mu\text{m}$  Chl *a* size fraction also showed significant dependence on light, although the adjusted  $r^2$  value of this model was only 0.296, indicating meager dependence. We included pDA in our MLR analysis as a predictor variable due to its potential to enhance acquisition of trace metals necessary for nitrate reduction and metabolic enzymes. However, the concentration of pDA did not significantly predict *P-n* spp. growth.

**In situ grazing mortality of *Pseudo-nitzschia* and microzooplankton biomass**—Microzooplankton grazing rates on *P-n* spp. varied considerably over the course of the study, ranging from 0 to  $1.70\text{ d}^{-1}$  (Fig. 3), and rates averaged  $0.32\text{ d}^{-1}$  across all years ( $n = 36$ ; Table 3). Highest *P-n* spp. grazing rates were measured in Sep 2003 and corresponded to the highest *P-n* spp. growth rates (Fig. 2). The grazing rates on *P-n* spp. in 2003 were, on average, higher than either of the Chl *a* size fractions (Table 3). Grazing rates on *P-n* spp. in Sep 2004 and pooled Jun and Sep 2005 grazing rates were significantly lower than 2003 rates (Kruskal–Wallis ANOVA,  $p = 0.007$ ; Table 3), and most rates were  $\leq 0.25\text{ d}^{-1}$ . Lowest sustained *P-n* spp. grazing rates were found within the Juan de Fuca eddy bloom (see Table 1 for experiments) in 2004 (Fig. 3). Microzooplankton grazing rates were, on average, highest on the  $<5\text{-}\mu\text{m}$  Chl *a* size fraction (Table 3) and statistically greater (Kruskal–Wallis ANOVA on ranks,  $p < 0.05$ ) than grazing rates experienced by *P-n* spp. and the  $>5\text{-}\mu\text{m}$  Chl *a* size fraction, which were statistically equal (Kruskal–Wallis ANOVA on ranks,  $p < 0.05$ ).

The biomass and abundance of the dominant microzooplankton functional groups varied in both time and space (Fig. 4). The highest average microzooplankton abundance was seen in Sep of 2004 (Table 5), coincident with the maximal concentrations of *P-n* spp. observed during this 3-yr study (Table 2). When heterotrophic nanoflagellates, which are recognized to be near obligate grazers of nano- and picoplankton (e.g., Sherr and Sherr

1994), are omitted, the majority of this increase in abundance is from ciliates ( $<40\text{ }\mu\text{m}$ ) and the larger ( $>40\text{ }\mu\text{m}$ ) gymnodinoid heterotrophic dinoflagellates (Fig. 4). On average, across all years, the abundance of heterotrophic dinoflagellates was greater than that of ciliates (Table 5).

The mean microzooplankton biomass was remarkably similar across years, averaging 40.0, 37.5, 34.6, and  $41.0\text{ }\mu\text{g C L}^{-1}$  for 2003, 2004, and 2005 Jul and Sep, respectively (Table 5). With the exception of Sep 2005, when biomass of heterotrophic dinoflagellates was near  $2\times$  higher than biomass of ciliates, biomass estimates of these two functional groups were similar (Table 5).

*P-n*-specific grazing rates did not correlate with either total microzooplankton abundance ( $r^2 = -0.32$ ,  $p > 0.05$ ) or biomass ( $r^2 = -0.18$ ,  $p \gg 0.05$ ). However, within the microzooplankton community, there exist numerous functional feeding groups that are unlikely to graze on *P-n* spp. or other diatoms. As such, the use of total microzooplankton biomass or abundance in analyses may obscure a possible relationship with *P-n* grazing. Consequently, the biomasses of several microzooplankton functional groups were tested for correlations with *P-n* spp. grazing (Table 6). The biomass of  $<40\text{-}\mu\text{m}$ -sized *Gymnodinium*-like heterotrophic dinoflagellates was the only functional group that positively correlated with *P-n* spp. grazing rate. Heterotrophic nanoflagellate biomass correlated with *P-n* spp. grazing, but this correlation was negative.

## Discussion

This study was conducted to explore how selective forces that simultaneously affect both the growth and mortality environment select for the seemingly competitive advantage that *P-n* spp. often display over other phytoplankton, especially other diatoms. These advantages are exemplified by their wide geographic distribution, temporal persistence, and ability to numerically dominate phytoplankton blooms. Our findings contradict the paradigm that diatoms—especially when considering factors that regulate optimal growth—constitute an invariable functional group, and instead emphasize the uniqueness of *P-n* spp., showing that they are physiologically dissimilar to most other diatoms. Indirect evidence to support this claim can be seen in the relationship between *P-n* spp. biomass to that of total phytoplankton biomass. Typically, and particularly in coastal upwelling environments, the relative proportion of larger phytoplankton (usually diatoms) increases as total phytoplankton biomass increases (Chisholm 1992; Strom et al. 2007). It would then be expected that the diatom-dominated, high biomass observed on the PNW coast would be reflected in a proportional increase in *P-n* spp. This, however, was not the case; *P-n* spp. biomass did not correlate with total phytoplankton biomass (expressed as Chl *a* ( $r^2 = 0.04$ ,  $p = 0.814$ ), which indicates that factors selecting for the accumulation of most diatoms differ from factors that select for accumulation of *P-n* spp.

***Pseudo-nitzschia* growth**—*P-n* spp. intrinsic growth rates measured during this study were found to be consistently

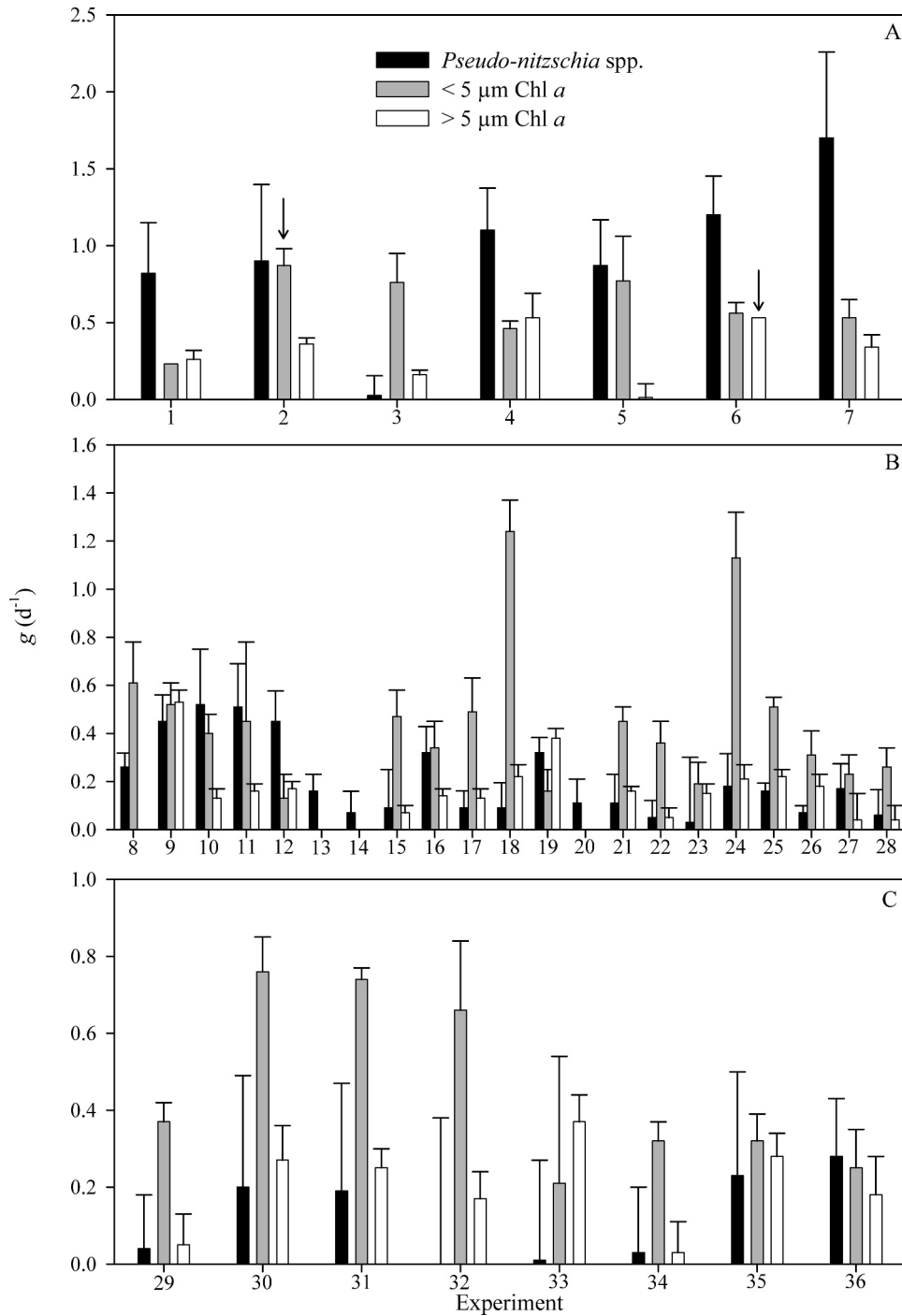


Fig. 3. Microzooplankton grazing rates ( $g$ ,  $d^{-1}$ ) on *P-n* spp.,  $<5 \mu m$  Chl  $a$ , and  $>5 \mu m$  Chl  $a$  for (A) 2003, (B) 2004, and (C) Jul (exp. 29–31) and Sep (exp. 32–36) 2005. Error bars are the standard error of the slope from each dilution experiment regression. Arrows indicate size fractions and experiments where saturated grazing kinetics were observed. Grazing rates during these experiments were corrected according to methods section. Note the change in scale of the ordinal axis for each plot.

high: maximum rates neared  $2.30 d^{-1}$  (Fig. 2). These rates are higher than published intrinsic growth rates for cultured *P-n* spp. but well within the range of growth rates for similar-sized diatoms calculated using the allometric relationship  $\mu_{max} = 3.4V^{-0.13}$  (cf. review by Sarthou et al.

2005). What is perhaps most interesting with regard to our *P-n* spp. intrinsic growth rates is that (1) consistently high intrinsic growth rates were maintained across wide-ranging physical and macronutrient concentrations, including low and undetectable nitrate concentrations (Fig. 5), and (2) *P-*

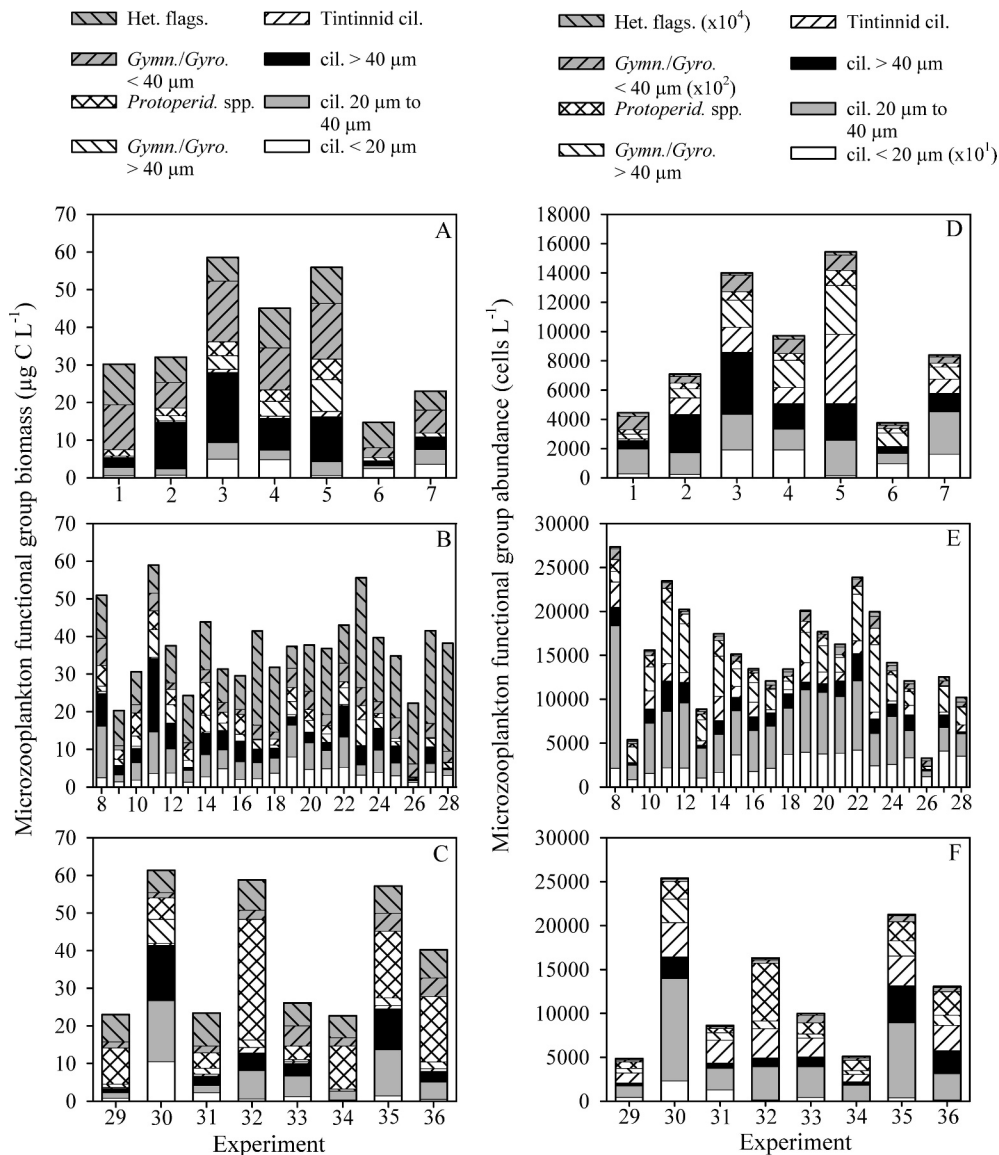


Fig. 4. The initial biomass and abundance of the major microzooplankton functional groups from dilution experiments in (A,D) 2003, (B,E) 2004, and (C,F) 2005. Note the change in scale of the ordinal axis in (panel D). The abundances of several microzooplankton functional groups are expressed in different magnitudes. Het. flags., heterotrophic nanoflagellates; *Gymn./Gyro.*, Gymnodinium-like heterotrophic dinoflagellates; *Protopterid.*, *Protopteridinium* spp.; cil., ciliates.

*n* spp. grew at rates exceeding those of the Chl *a* communities, and most surprisingly, faster than the  $<5\text{-}\mu\text{m}$  Chl *a* size fraction (Table 3). In general, small cells grow comparatively faster than large cells in culture studies (Tang 1995) and are less constrained by resource limitation than large cells (Chisholm 1992). However, these size-based allometric relationships do not always hold true in situ (Kagami and Urabe 2001), highlighting the importance of the interactive effects that concurrent selective forces have on algal growth physiology. The finding here that *P-n* spp. grew consistently faster than these small phytoplankton implies that the growth physiology of *P-n* spp. is, compared to most other phytoplankton, better suited to tolerate conditions when resources are limiting.

The observed moderate to high *P-n* spp. growth at low to undetectable nitrate was a trend that was supported by our MLR model; nitrate concentration did not significantly predict *P-n* spp. growth. This contrasts with the  $<5\text{-}\mu\text{m}$  and  $>5\text{-}\mu\text{m}$  Chl *a* size fractions, both of which showed dependence on nitrate for growth. Although *P-n* spp. cells can ostensibly be considered large phytoplankton, with individuals ranging in length from  $50 \mu\text{m}$  to  $170 \mu\text{m}$ , the narrow pennate morphology of *P-n* spp. results in a very high surface area-to-volume ratio, making the cells quite conducive to growth at low nutrient concentrations, and functionally similar to small phytoplankton. To illustrate this, the average ( $n = 600$ ) equivalent spherical diameter of *P-n* spp. from several of our experiments was  $\sim 7 \mu\text{m}$ . With

Table 5. Average initial microzooplankton abundance and biomass for each year and month of our study. The range of values is shown in parenthesis. H, heterotrophic.

Year	Ciliate		H. dinoflagellate		H. nanoflagellate		Total	
	Abundance (cells mL <sup>-1</sup> )	Biomass (µg C L <sup>-1</sup> )	Abundance (cells mL <sup>-1</sup> )	Biomass (µg C L <sup>-1</sup> )	Abundance (cells mL <sup>-1</sup> )	Biomass (µg C L <sup>-1</sup> )	Abundance (cells mL <sup>-1</sup> )	Biomass (µg C L <sup>-1</sup> )
2003								
September (n=7)	15.6 (5.5–27.7)	14.2 (4.6–28.9)	77.0 (26.4–116.1)	15.6 (6.4–28.7)	1,673 (1,198–2,073)	10.2 (7.3–12.6)	1,765 (1,323–2,139)	40.0 (23.4–61.0)
2004								
September (n=21)	35.6 (10.9–54.8)	13.7 (2.3–34.6)	64.6 (28.7–142.7)	9.2 (4.0–17.1)	2,407 (938–4,778)	14.6 (5.7–29.1)	2,507 (1,105–4,951)	37.5 (20.3–58.9)
2005								
July (n=3)	22.7 (7.7–41.6)	17.7 (3.8–42.1)	25.1 (20.8–30.9)	11.0 (7.5–13.4)	765 (485–1,030)	5.8 (5.1–6.7)	813 (557–1,061)	34.6 (20.0–61.2)
September (n=5)	11.2 (3.8–20.4)	13.6 (8.6–25.6)	58.0 (30.1–92.7)	21.8 (10.4–36.2)	1,217 (1,037–1,504)	6.8 (5.7–7.8)	1,287 (1,114–1,560)	41.0 (25.5–58.5)
Average (n=36)	22.1	14.8	56.2	14.4	1,515	9.4	1,593	38.5

an equivalent radius of 3.5 µm, *P-n* spp. growing rapidly at 1.50 d<sup>-1</sup> would require a threshold N concentration of only ~0.08 µmol L<sup>-1</sup> before growth would be diffusion-limited by N (Chisholm 1992). In terms of nutrient diffusion, this morphological characteristic places *P-n* spp. functionally in the category of the smallest of the nanoplankton (2.0 to 20 µm). However, because *P-n* spp. exhibited high growth rates at undetectable to low nitrate concentrations, *P-n* spp. must also have the ability to adequately use N sources other than nitrate for sustained high growth. Indeed, it has been shown that both the larger cell-sized *P. australis* and the much smaller cell-sized *P. cf. cuspidata* can grow equally well on nitrate or ammonium when either is supplied as the sole N source under saturating N and PAR, whereas urea supports slower average growth (Auro 2007; Howard et al. 2007). Ammonium concentrations across our study region were consistently low (<0.2 µmol L<sup>-1</sup>; Cochlan unpubl.), but ammonium turnover rates were not measured in our experiments. Therefore, the degree to which *P-n* spp. were sustained by ammonium in this region remains unknown.

Table 6. Correlation coefficients and *p* values for the association between microzooplankton functional group biomass and *P-n* spp. grazing rate. Significant correlations are denoted by \*\*. Cil., ciliates; H., heterotrophic.

Microzooplankton functional group	Correlation with <i>Pseudo-nitzschia</i> spp. grazing	
	<i>r</i> <sup>2</sup>	<i>p</i>
Cil. <20 µm	-0.059	0.733
Cil. 20–40 µm	-0.180	0.294
Cil. >40 µm	-0.113	0.511
Tintinnid cil.	0.033	0.845
H. nanoflagellates	-0.345	0.040**
H. gymnodinoids <40 µm	0.338	0.043**
H. gymnodinoids >40 µm	0.040	0.819
<i>Protoperidinium</i> spp.	-0.232	0.173

*P-n* spp. independence from nitrate for sustained rapid growth may be a physiological adaptation and not simply a by-product resulting from a high surface area-to-volume ratio; Cochlan et al. (in press) demonstrated that N-starved *P. cf. delicatissima* can take up ammonium at amplified rates that exceed N quotas for exponential growth. This transient (surge) uptake ability may provide *P. cf. delicatissima*, and perhaps other *P-n* spp. with a competitive advantage during periods when marine ecosystems are operating under N-limited conditions.

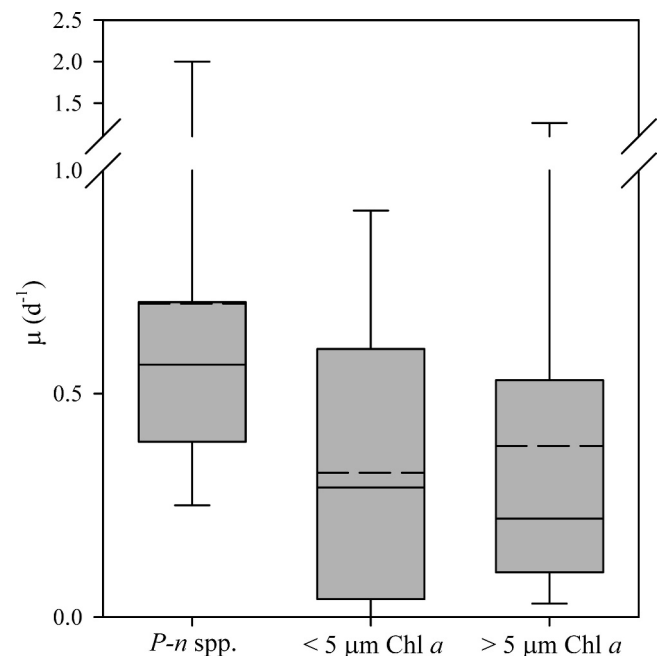


Fig. 5. Intrinsic growth rates of *P-n* spp., <5 µm Chl *a*, and >5 µm Chl *a* at nitrate concentrations <1 µmol L<sup>-1</sup>. Box plots show the median (solid line), mean (dashed line), and upper and lower quartiles. Whiskers show the lower 5th and upper 95th percentiles.

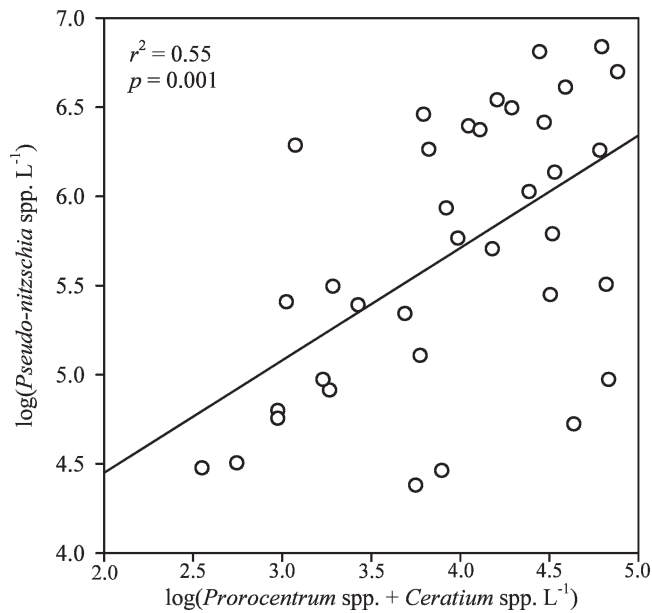


Fig. 6. A log vs. log scatter plot showing the correlation between *P-n* spp. abundance and the combined abundance of the large autotrophic dinoflagellates, *Prorocentrum* spp. and *Ceratium* spp.

The disparity in nutrient physiology between *P-n* spp. and the Chl *a* size fractions is further made apparent by observing that *P-n* spp. did not show evidence of nutrient limitation during our incubations (Fig. 2). This contrasts with both size fractions of Chl *a*, which often showed evidence for nutrient stress by responding positively to nutrient (including Fe) addition in our dilution controls (Fig. 2). In many cases, ambient macronutrient concentrations were quite high (Table 1) and, for the levels of in situ phytoplankton biomass (Table 2), should have been sufficient to support high growth rates during the incubations. This fact supports the notion that at times the PNW coast may—like other coastal upwelling (Hutchins et al. 1998; Bruland et al. 2001) and productive environments (Strom et al. 2007)—experience micronutrient (presumably Fe) limitation. *P-n* spp. were not macronutrient limited under these conditions, supporting laboratory (Maldonado et al. 2002; Wells et al. 2005) and field data (Wells et al. 2005; Marchetti et al. 2006a) that show that *P-n* spp. have unique strategies to cope with Fe stress.

Another interesting output of our MLR model was that, unlike the  $>5\text{-}\mu\text{m}$  Chl *a* size fraction, *P-n* spp. intrinsic growth was dependent upon high irradiance. Coastal diatoms typically dominate during more turbulent conditions when inorganic nutrients are being supplied at high rates (Sarhou et al. 2005). Under these conditions, total irradiance received per cell over time is lower compared to more quiescent conditions as a result of deeper vertical mixing. Our finding that *P-n* spp. are dependent upon high light is especially significant when coupled with the finding that *P-n* spp. can grow at high in situ rates at undetectable or low nitrate; this implies that the temporal persistence of *P-n* spp. may stem from an ability to grow well in stratified

conditions (e.g., Trainer et al. 2007). Indeed, *P-n* spp. biomass was positively correlated ( $p = 0.001$ ,  $r^2 = 0.55$ ; Fig 6) with the abundance of the large, autotrophic dinoflagellates *Ceratium* spp. and *Prorocentrum* spp.—two phytoplankton genera typically associated with stratified, late successional stages (Smayda 1980). Evidence that supports our finding that *P-n* spp. are at least tolerant to stratification includes the recent blooms of *P-n* spp. found in strongly stratified enclosed bays in Washington State, U.S.A. (Trainer et al. 2007), and the fact that *P-n* spp. do not appear to be as sensitive to ultraviolet (UV), especially UVA, compared to other algal species (e.g., Mengelt and Prézelin 2005).

The MLR analysis also indicated a significant negative relationship between *P-n* growth rate and temperature. Since upwelled water is both cold and high in nutrients, this relationship may reflect an indirect, rather than direct, effect of temperature. However, our MLR analysis did not show collinearity between either the 24-h incubator temperature or the in situ water temperature and nitrate, and the MLR analysis did not reveal a significant relationship between nitrate and *P-n* growth rate. Therefore, it is unlikely that the negative temperature–growth relationship is based on elevated nitrate levels in colder, more recently upwelled water. It is possible that temperature is a proxy for a limiting nutrient or inhibitor, specific to *P-n*, that was not examined. Since the temperature range at which phytoplankton species grow maximally is typically quite narrow ( $\sim 3^\circ\text{C}$ ; Montagnes et al. 2003), it is also possible that the temperatures encountered during this study and in our incubations may have exceeded the optimal growth temperatures for the *P-n* spp. present in our experiments.

*Microzooplankton grazing on Pseudo-nitzschia*—Microzooplankton community grazing rates on *P-n* spp. measured in this study were most often low, but they were comparable in range to grazing on other, large ( $>5\ \mu\text{m}$ ) phytoplankton (Fig. 3; Table 3). There were a few exceptions, most notably Sep 2003, but even when grazing rates were moderately high, the corresponding *P-n* spp. growth rates were considerably higher (Fig. 7), indicating that microzooplankton grazing affects the population ecology of *P-n* spp. minimally. The lack of a strong grazing control on *P-n* populations was particularly apparent during the Sep 2004 Juan de Fuca eddy bloom (Lessard et al. unpubl.). The bloom, which lasted at least 11 d and contained the highest abundances of *P-n* spp. cells (Table 2), corresponded to the lowest measured *P-n* spp. intrinsic growth rates during this study (Table 3), indicating that mortality during this bloom event was minimal.

Although microzooplankton grazing can substantially reduce the rate of accumulation of large phytoplankton, specifically diatoms (e.g., Neuer and Cowles 1994; Strom et al. 2001), microzooplankton grazing rarely balances intrinsic growth rates for these large cells. A likely reason for this uncoupling is the high prey specificity of diatom-consuming microzooplankton. These microzooplankton, which can be much smaller than their prey, including *P-n* spp., have very specialized feeding behaviors (e.g., Hansen

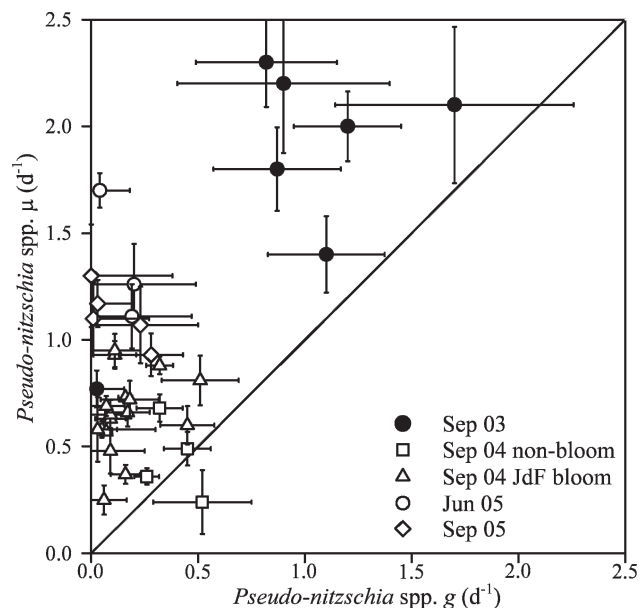


Fig. 7. *P-n* spp. intrinsic growth rates ( $\mu$ ,  $\text{d}^{-1}$ ) plotted against intrinsic microzooplankton grazing rates ( $g$ ,  $\text{d}^{-1}$ ) for 36 in situ experiments conducted in the coastal Pacific Northwest. Line bisecting graph represents equal rates. Error bars are standard error of the slope and intercept from dilution regressions. JdF, Juan de Fuca eddy.

and Calado 1999); consequently, ingestion of diatoms is restricted to specific grazer functional groups. Therefore, even if microzooplankton biomass is high, if microzooplankton species that possess an affinity or ability to graze on *P-n* spp. are in low abundance, this may ease grazing pressure and provide the loophole (Irigoien et al. 2005) necessary for *P-n* bloom formation. This hypothesis is indirectly supported by this study; although the total microzooplankton biomass did not correlate with *P-n* spp. grazing, we found a correlation between heterotrophic gymnodinoid dinoflagellates  $<40 \mu\text{m}$  in size, a grazer capable of ingesting larger diatoms, and grazing rates on *P-n* spp. (Table 6).

Microzooplankton often demonstrate selective feeding behavior (Verity 1991), and, as such, a second possible reason *P-n* spp. escape intense grazing may be related to microzooplankton avoidance of less desirable prey. *P-n* spp. provide little C  $\text{cell}^{-1}$  when compared to other, often abundant, diatom prey. Table 7 shows the number of prey cells required for growth of three different types of heterotrophic dinoflagellates when feeding on several potential diatom prey species. The number of *P-n* spp., small or large, required for one division for these three microzooplankton is much higher than for other available diatoms. Therefore, grazing on *P-n* spp. when other large prey are available is not energetically favorable and may lead to avoidance of *P-n* spp. by microzooplankton grazers that otherwise are capable of ingesting these pennate diatoms. Although this argument is defensible based on energetics, it does not explain why the larger phytoplankton size fraction was grazed at relatively low rates equal to *P-n* spp.

Another possible reason for relatively low *P-n* grazing rates is that DA, like other marine phytoplankton secondary metabolites, may act as a chemical signaling molecule that retards zooplankton grazing (Wolfe 2000 and references therein). However, we found no evidence of this in the present study; correlations were insignificant between *P-n*-specific grazing and pDA and dDA (data not shown). Further, in parallel dilution experiments with and without added dDA (up to  $80 \text{ nmol L}^{-1}$ ), grazing rates between treatments were statistically the same (Olson et al. unpubl.). DA has also been found to have no effect on calanoid copepod grazing in this region (Olson et al. 2006).

*Balance between growth and grazing and its ecological significance*—In order to gauge the comprehensive competitive fitness of an organism, the intrinsic rates of growth and mortality must be measured under the multitude of diverse, yet integrated, selective pressures operating in its environment. The optimum life-history strategy for any organism would be to maximize fecundity and reduce mortality at all life stages (Gotelli 2001) and under all environmental conditions. Although this assumption is

Table 7. Number of ingested prey cells required for three different microzooplankton grazers to divide one time assuming gross growth efficiency (GGE) of 30%. Grazer and prey C estimates were calculated from initial cell counts from several random experiments, except *D. brightwellii*, which came from laboratory cultures (data not shown). I.D., ingestion demand. Small (s) and large (L) *P-n* spp. values were calculated as in methods section.

Grazer	pg C grazer <sup>-1</sup>	Prey species	pg C cell <sup>-1</sup> ± SE	I.D. (cells) with 30% GGE
<i>Gyrodinium</i> cf. <i>spirale</i>	886 ± 104 (n=400)	<i>Pseudo-nitzschia</i> spp. (s)	10.7 ± 0.5 (n=200)	275.7
		<i>Pseudo-nitzschia</i> spp. (L)	85.0 ± 4.1 (n=91)	34.7
		<i>Thalassiosira</i> spp.	225.0 ± 14.8 (n=200)	13.1
		<i>Ditylum brightwellii</i>	824.0 ± 37.0 (n=100)	3.6
<i>Protoperidinium</i> spp.	4,880 ± 774 (n=400)	<i>Pseudo-nitzschia</i> spp. (s)	10.7 ± 0.5 (n=200)	1,518.7
		<i>Pseudo-nitzschia</i> spp. (L)	85.0 ± 4.1 (n=91)	191.2
		<i>Thalassiosira</i> spp.	225.0 ± 14.8 (n=200)	72.2
		<i>Ditylum brightwellii</i>	824.3 ± 37.0 (n=100)	19.7
Gymnodinoids $<40 \mu\text{m}$	73 ± 4 (n=200)	<i>Pseudo-nitzschia</i> spp. (s)	10.7 ± 0.5 (n=200)	22.7
		<i>Pseudo-nitzschia</i> spp. (L)	85.0 ± 4.1 (n=91)	2.9
		<i>Thalassiosira</i> spp.	225.0 ± 14.8 (n=200)	1.1
		<i>Ditylum brightwellii</i>	824.3 ± 37.0 (n=100)	0.3

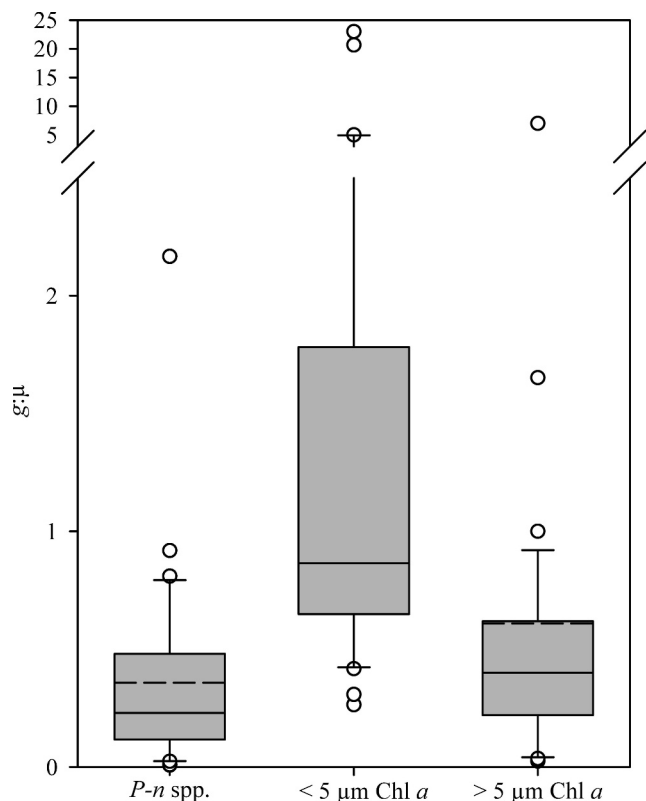


Fig. 8. Ratios of  $g:\mu$  for *P-n* spp.,  $<5\text{-}\mu\text{m}$  aggregate Chl *a*, and  $>5\text{-}\mu\text{m}$  aggregate Chl *a*. Box plots show the median (solid line), mean (dashed line), and upper and lower quartiles. Whiskers are the lower 10th and upper 90th percentiles. Open circles represent potential outliers. Due to extreme outliers for the  $<5\text{-}\mu\text{m}$  Chl *a* size fraction, the mean is above the upper quartile and thus not visible.

relative to the number of life-history stages an organism undergoes, the principle applies to all living organisms, including single-celled eukaryotic phytoplankton. The strong competitive fitness of *P-n* spp. and, ultimately, their success on the PNW coast likely result from exploiting just such a strategy, analogous to expression of a continuum of  $r$  (e.g., fast growing) and  $K$  (e.g., low mortality) selection strategies (MacArthur and Wilson 1967).

The effect of grazing on the demographics of a phytoplankton population becomes increasingly important when grazing rate ( $g$ ) becomes similar to the phytoplankton specific growth rate ( $\mu$ ). We found that  $g:\mu$  ratios for *P-n* spp. are, on average, lower than both communities of size-fractionated Chl *a* (Fig. 8). Since these ratios were measured across diverse growth conditions, barring other significant loss sources, these low  $g:\mu$  ratios for *P-n* spp. will lead to higher rates of accumulation in the environment. Since mesozooplankton were excluded from our experiments, the  $g:\mu$  ratios reported here are potentially underestimates. However, copepods from this same study region were found to generally avoid ingesting *P-n* spp., and copepod community grazing impact on *P-n* production was estimated to be only  $\sim 10\%$  of *P-n* production (Olson et al. 2006). Instead, copepods preferentially grazed on the microzoo-

plankton, specifically, the functional group shown in this study to graze significantly on *P-n* spp. (Table 6). Therefore, our reported low  $g:\mu$  ratios for *P-n* spp. could in fact be potential overestimates. Our experiments were done only in surface waters (3–5 m), and it is possible that depth-integrated  $g:\mu$  ratios might be higher as phytoplankton growth is reduced by light attenuation with depth. However, even if higher  $g:\mu$  ratios are found for *P-n* spp. at deeper depths, it has little bearing on the conclusions of this study; across our study region where *P-n* was present, on average 78% of *P-n* abundance ( $n = 27$ ) was found in the upper 5 m, and few to no *P-n* spp. were found below 10 m (Trainer et al. unpubl.), where growth would likely be limited.

In light of lower  $g:\mu$  ratios for *P-n* spp. compared to the other phytoplankton populations, it is judicious to ask why *P-n* spp. were not present and the dominant species in all discrete samples across the PNW region. First, the Chl *a*-based rates used in this study are the aggregate averages of rates of individual populations. It is likely that even though *P-n* spp. grew consistently at moderate to high rates, and at rates consistently higher than both of the aggregate Chl *a* size fractions, there were other phytoplankton that were growing faster, but their individual rates were masked by the community-wide aggregate measure. Second, there are other sources of loss acting on *P-n* spp., both biotic (e.g., viruses, parasites, autolysis, aggregation) and abiotic (e.g., advection, subduction), which we did not address. Understanding how these other factors, especially the abiotic ones, affect the population ecology of *P-n* spp. is important, but they are difficult to quantify due to the ephemeral and infrequent nature of these events. Finally, in order to explore which factors most influence the population ecology of *P-n* spp., it was necessary to collect water from locations where *P-n* spp. were present and, to satisfy statistical assumptions, moderately abundant. During this three-year study, these conditions were met in 68% (range 46% to 91%) of the multiple samplings at the 123 ECOHAB-PNW sampling stations (Trainer unpubl.). Therefore, locations did exist in our study region where *P-n* spp. were not present, leaving open the question: what are the environmental conditions necessary to initiate a population of *P-n* spp.?

In summary, we have shown that *P-n* spp. in surface waters consistently grow at moderate to high rates under wide-ranging environmental conditions and that mortality from microzooplankton grazing is almost always lower than growth rate. Thus, this toxigenic diatom appears to have evolved a life-history strategy that maximizes growth and reduces grazing mortality, potentially placing it at a competitive advantage over other phytoplankton in the coastal Pacific Northwest. Further, this successful life-history pattern likely contributes to the prevalence of *P-n* spp., not only in the PNW, but also in their global ocean distribution.

## References

- ADAMS, N. G., M. LESOING, AND V. L. TRAINER. 2000. Environmental conditions associated with domoic acid in razor clams on the Washington coast. *J. Shellfish Res.* **19**: 1007–1015.

- AURO, M. E. 2007. Nitrogen dynamics and toxicity of the pennate diatom *Pseudo-nitzschia cuspidata*: A field and laboratory based study. M.S. thesis, San Francisco State Univ.
- BANSE, K. 1994. Grazing and zooplankton production as key controls of phytoplankton production in the open ocean. *Oceanography* **7**: 13–20.
- BATES, S. S., D. L. GARRISON, AND R. A. HORNER. 1998. Bloom dynamics and physiology of domoic-acid producing *Pseudo-nitzschia* species, p. 267–292. In G. M. Hallegraeff [ed.], *Physiological ecology of harmful algal blooms*. Springer-Verlag.
- , AND V. L. TRAINER. 2006. The ecology of harmful diatoms. *Ecol. Stud.* **189**: 81–93.
- BRULAND, K. W., E. L. RUE, AND G. J. SMITH. 2001. Iron and macronutrients in California coastal upwelling regimes: Implications for diatom blooms. *Limnol. Oceanogr.* **46**: 1661–1674.
- CALBET, A., AND M. R. LANDRY. 2004. Phytoplankton growth, microzooplankton grazing, and carbon cycling in marine systems. *Limnol. Oceanogr.* **49**: 51–57.
- CHISHOLM, S. W. 1992. Phytoplankton size, p. 213–237. In P. G. Falkowski and A. D. Woodhead [eds.], *Primary productivity and biogeochemical cycles in the sea*. Plenum.
- COCHLAN, W. P., J. HERNDON, AND R. M. KUDELA. In press. Inorganic and organic nitrogen uptake by the toxigenic diatom *Pseudo-nitzschia australis* (Bacillariophyceae). *Harmful Algae*.
- DOLAN, J. R., AND K. MCKEON. 2004. The reliability of grazing rate estimates from dilution experiments: Have we overestimated rates of organic carbon consumption by microzooplankton? *Ocean Sci. Disc.* **1**: 1–7.
- FIRST, M. R., P. J. LAVRENTYEV, AND F. J. JOCHEM. 2007. Patterns of microzooplankton growth in dilution experiments across a trophic gradient: Implications for herbivory studies. *Mar. Biol.* **151**: 1929–1940.
- FROST, B. W. 1991. The role of grazing in nutrient-rich areas of the open sea. *Limnol. Oceanogr.* **36**: 1616–1630.
- GALLEGOS, C. L. 1989. Microzooplankton grazing on phytoplankton in the Rhode River, Maryland: Nonlinear feeding kinetics. *Mar. Ecol. Prog. Ser.* **57**: 23–33.
- GOTELLI, N. J. 2001. *A primer of ecology*. Sinauer Associates.
- HANSEN, P. J., AND A. J. CALADO. 1999. Phagotrophic mechanisms and prey selection in free-living dinoflagellates. *J. Eukaryot. Microbiol.* **46**: 382–389.
- HICKEY, B. M., AND N. S. BANAS. 2003. Oceanography of the US Pacific Northwest coastal ocean and estuaries with application to coastal ecology. *Estuaries* **26**: 1010–1031.
- HORNER, R. A. 2002. A taxonomic guide to some common marine phytoplankton. Biopress.
- , B. M. HICKEY, AND J. R. POSTEL. 2000. *Pseudo-nitzschia* blooms and physical oceanography off Washington State, USA. *S. Afr. J. Mar. Sci.* **22**: 299–308.
- HOWARD, M. D. A., W. P. COCHLAN, N. LADIZINSKY, AND R. M. KUDELA. 2007. Nitrogenous preference of toxigenic *Pseudo-nitzschia australis* (Bacillariophyceae) from field and laboratory experiments. *Harmful Algae* **6**: 206–217.
- HUTCHINS, D. A., G. R. DITULLIO, Y. ZHANG, AND K. W. BRULAND. 1998. An iron limitation mosaic in the California upwelling regime. *Limnol. Oceanogr.* **43**: 1037–1054.
- IRIGOIEN, X., K. J. FLYNN, AND R. P. HARRIS. 2005. Phytoplankton blooms: A 'loophole' in microzooplankton grazing impact? *J. Plankton Res* **27**: 313–321.
- KAGAMI, M., AND J. URABE. 2001. Phytoplankton growth rate as a function of cell size: An experimental test in Lake Biwa. *Limnol.* **2**: 111–117.
- KNEPEL, K., AND K. BOGREN. 2002. Determination of orthophosphate by flow injection analysis: QuickChem Method 31-115-01-1-H, 12 p. In *Methods manual*. Lachat Instruments.
- LANDRY, M. R., AND A. CALBET. 2004. Reality checks on microbial food web interactions in dilution experiments: Responses to the comments of Dolan and McKeon. *Ocean Sci. Disc.* **1**: 65–76.
- , J. CONSTANTINOU, AND J. KIRSSTEIN. 1995. Microzooplankton grazing in the central Equatorial Pacific during February and August, 1992. *Deep-Sea Res. II* **42**: 657–671.
- LESSARD, E. J., AND M. C. MURRELL. 1996. Distribution, abundance and size composition of heterotrophic dinoflagellates and ciliates in the Sargasso Sea near Bermuda. *Deep-Sea Res. I* **43**: 1045–1065.
- MACARTHUR, R., AND E. O. WILSON. 1967. *The theory of island biogeography*. Princeton Univ. Press.
- MACFADYEN, A., B. M. HICKEY, AND W. P. COCHLAN. In press. Influences of the Juan de Fuca eddy on circulation, nutrients and phytoplankton production in the Northern California Current System *J. Geophys. Res.*
- MALDONADO, M. T., M. P. HUGHES, E. L. RUE, AND M. L. WELLS. 2002. The effect of Fe and Cu on growth and domoic acid production by *Pseudo-nitzschia multiseriis* and *Pseudo-nitzschia australis*. *Limnol. Oceanogr.* **47**: 515–526.
- MARCHETTI, A., AND P. J. HARRISON. 2007. Coupled changes in the cell morphology and the elemental (C, N and Si) composition of the pennate diatom *Pseudo-nitzschia* due to iron deficiency. *Limnol. Oceanogr.* **52**: 2270–2284.
- , M. T. MALDONADO, E. S. LANE, AND P. J. HARRISON. 2006a. Iron requirements of the pennate diatom *Pseudo-nitzschia*: Comparison of oceanic (high-nitrate, low-chlorophyll waters) and coastal species. *Limnol. Oceanogr.* **51**: 2092–2101.
- , N. D. SHERRY, J. PHILIPPE, R. F. STRZEPEK, AND P. J. HARRISON. 2006b. Phytoplankton processes during a meso-scale iron enrichment in the NE subarctic Pacific: Part 1. Biomass and assemblage. *Deep-Sea Res. II* **53**: 2095–2113.
- MENDEN-DEUER, S., AND E. J. LESSARD. 2000. Carbon to volume relationships for dinoflagellates, diatoms, and other protist plankton. *Limnol. Oceanogr.* **45**: 569–579.
- MENGELT, C., AND B. B. PRÉZELIN. 2005. UVA enhancement of carbon fixation and resilience to UV inhibition in the genus *Pseudo-nitzschia* may provide a competitive advantage in high UV surface waters. *Mar. Ecol. Prog. Ser.* **301**: 81–93.
- MONTAGNES, D. J. S., S. A. KIMMANCE, AND D. ATKINSON. 2003. Using Q10: Can growth rates increase linearly with temperature? *Aquat. Microb. Ecol.* **32**: 307–313.
- NETER, J., M. H. KUTNER, C. J. NACHTSHEIM, AND W. WASSERMAN. 1996. *Applied linear regression models*, 3rd ed. McGraw-Hill.
- NEUER, S., AND T. J. COWLES. 1994. Protist herbivory in the Oregon upwelling system. *Mar. Ecol. Prog. Ser.* **113**: 147–162.
- OLSON, M. B., E. LESSARD, C. H. J. WONG, AND M. J. BERNHARDT. 2006. Copepod feeding selectivity on microplankton, including the toxigenic diatoms *Pseudo-nitzschia* spp., in the coastal Pacific Northwest. *Mar. Ecol. Prog. Ser.* **326**: 207–220.
- PARSONS, T. R., Y. MAITA, AND C. M. LALLI. 1984. *A manual of chemical and biological methods for seawater analysis*. Pergamon.
- PERL, T. M., L. BEDARD, T. KOSATSKY, J. C. HOCKIN, E. C. D. TODD, AND R. S. REMIS. 1990. An outbreak of toxic encephalopathy caused by eating mussels contaminated with domoic acid. *N. Eng. J. Med.* **322**: 1775–1780.
- PUTT, M., AND D. K. STOECKER. 1989. An experimentally determined carbon: volume ratio for marine "oligotrichous" ciliates from estuarine and coastal waters. *Limnol. Oceanogr.* **34**: 1097–1103.

- ROFF, J. C., AND R. R. HOPCROFT. 1986. High precision microcomputer based measuring system for ecological research. *Can. J. Fish. Aquat. Sci.* **43**: 2044–2048.
- RUE, E., AND K. BRULAND. 2001. Domoic acid binds iron and copper: A possible role for the toxin produced by the marine diatom *Pseudo-nitzschia*. *Mar. Chem.* **76**: 127–134.
- SARTHOU, G., K. R. TIMMERMANS, S. BLAIN, AND P. TREGUER. 2005. Growth physiology and fate of diatoms in the ocean: A review. *J. Sea Res.* **53**: 25–42.
- SCHNETZER, A., P. E. MILLER, R. A. SCHAFFNER, B. A. STAUFFER, B. H. JONES, S. B. WEISBERG, P. M. DIGIACOMO, W. M. BERELSON, AND D. A. CARON. 2007. Blooms of *Pseudo-nitzschia* and domoic acid in the San Pedro Channel and Los Angeles harbor areas of the Southern California Bight. *Harmful Algae* **6**: 372–387.
- SCHOLIN, C. A., AND OTHERS. 2000. Mortality of sea lions along the central California coast linked to a toxic diatom bloom. *Nature* **403**: 80–84.
- SHERR, E. B., AND B. F. SHERR. 1994. Bacterivory and herbivory: Key roles of phagotrophic protists in pelagic food webs. *Microb. Ecol.* **28**: 223–235.
- SMAYDA, T. J. 1980. Phytoplankton species succession, p. 493–570. *In* I. Morris [ed.], *The physiological ecology of phytoplankton*. Univ. California Press.
- SMITH, P., AND K. BOGREN. 2001. Determination of nitrate and/or nitrite in brackish or seawater by flow injection analysis colorimetry: QuickChem Method 31-107-04-1-E, 12 p. *In* *Methods manual*. Lachat Instruments.
- STEHR, C. M., L. CONNELL, K. A. BAUGH, B. D. BILL, N. G. ADAMS, AND V. L. TRAINER. 2002. Morphological, toxicological, and genetic differences among *Pseudo-nitzschia* (Bacillariophyceae) species in inland embayments and outer coastal waters of Washington State, USA. *J. Phycol.* **38**: 55–65.
- STROM, S. L., M. A. BRAINARD, J. L. HOLMES, AND M. B. OLSON. 2001. Phytoplankton blooms are strongly impacted by microzooplankton grazing in coastal North Pacific waters. *Mar. Biol.* **138**: 355–368.
- , M. B. OLSON, E. L. MACRI, AND C. W. MORDY. 2007. Cross-shelf gradients in phytoplankton community structure, nutrient utilization, and growth rate in the coastal Gulf of Alaska. *Mar. Ecol. Prog. Ser.* **328**: 75–92.
- TANG, E. P. 1995. The allometry of algal growth rates. *J. Plankton Res.* **17**: 1325–1335.
- TRAINER, V. L., W. P. COCHLAN, A. ERICKSON, B. D. BILL, F. H. COX, J. A. BORCHERT, AND K. A. LEFEBVRE. 2007. Recent domoic acid closures of shellfish harvest areas in Washington State inland waterways. *Harmful Algae* **6**: 449–459.
- , B. M. HICKEY, AND R. A. HORNER. 2002. Biological and physical dynamics of domoic acid production off the Washington coast. *Limnol. Oceanogr.* **47**: 1438–1446.
- VAN DOLAH, F. M., T. A. LEIGHFIELD, B. L. HAYNES, D. R. HAMPSON, AND J. S. RAMSDELL. 1997. A microplate receptor assay for the amnesic shellfish poisoning toxin, domoic acid, utilizing a cloned glutamate receptor. *Anal. Biochem.* **245**: 102–105.
- VERITY, P. G. 1991. Feeding in planktonic protozoans: Evidence for non-random acquisition of prey. *J. Protozool.* **38**: 69–76.
- WELLS, M. L., C. G. TRICK, W. P. COCHLAN, M. P. HUGHES, AND V. L. TRAINER. 2005. Domoic acid: The synergy of iron, copper, and the toxicity of diatoms. *Limnol. Oceanogr.* **50**: 1908–1917.
- WELSCHMEYER, N. A. 1994. Fluorometric analysis of chlorophyll *a* in the presence of chlorophyll *b* and pheopigments. *Limnol. Oceanogr.* **39**: 1985–1992.
- WOLFE, G. V. 2000. The chemical defense ecology of marine unicellular plankton: Constraints, mechanisms, and impacts. *Biol. Bull.* **198**: 225–244.
- WOLTERS, M. 2002. Determination of silicate in brackish or seawater by flow injection analysis. QuickChem Method 31-114-27-1-D, 12 p. *In* *Methods manual*. Lachat Instruments.
- WORK, T. M., B. BARR, A. M. BEALE, L. FRITZ, M. A. QUILLIAM, AND J. L. C. WRIGHT. 1993. Epidemiology of domoic acid poisoning in brown pelicans (*Pelecanus occidentalis*) and Brandt's cormorants (*Phalacrocorax penicillatus*) in California. *J. Zoo Wild. Med.* **24**: 54–62.

Received: 5 September 2007

Accepted: 12 February 2008

Amended: 10 March 2008